WMRC Reports
Waste Management and Research Center

Field Study of Transit Time of Water and Tracers Through a Soil Liner

Keros Cartwright
Ivan G. Krapac
Samuel V. Panno
Bruce R. Hensel

Illinois State Geological Survey

About WMRC's Electronic Publications:

This document was originally published in a traditional format.

It has been transferred to an electronic format to allow faster and broader access to important information and data.

While the Center makes every effort to maintain a level of quality during the transfer from print to digital format, it is possible that minor formatting and typographical inconsistencies will still exist in this document.

Additionally, due to the constraints of the electronic format chosen, page numbering will vary slightly from the original document.

The original, printed version of this document may still be available.

Please contact WMRC for more information:

WMRC
One E. Hazelwood Drive
Champaign, IL 61820
217-333-8940 (phone)

www.wmrc.uiuc.edu

WMRC is a division of the Illinois Department of Natural Resources

Field Study of Transit Time of Water and Tracers Through a Soil Liner

by

Keros Cartwright, Ivan G. Krapac,
Samuel V. Panno, Bruce R. Hensel
Illinois State Geological Survey

Kenneth R. Rehfeldt
Illinois State Water Survey

ENR

HWRIC
TECHNOLOGY · SOCIETY · ENVIRONMENT

Field Study of Transit Time
of Water and Tracers Through
a Soil Liner

by

Keros Cartwright, Ivan G. Krapac, Samuel V. Panno, Bruce R. Hensel
Illinois State Geological Survey

Kenneth R. Rehfeldt
Illinois State Water Survey

Prepared for

Hazardous Waste Research and Information Center
One East Hazelwood Drive
Champaign, Illinois 61820

HWRIC Project Number HWR-88-047

CONTENTS

FIGURES

TABLES

ABSTRACT

A soil liner, 7.3 × 14.6 × 0.9 meters, was constructed using full-sized equipment. The liner pond was filled in April 1988, and the liner has been monitored continuously. Water infiltrating the liner was monitored by three methods: a total water balance; four large ring, sealed infiltrometers; and 32 small ring infiltrometers. Average infiltration fluxes of 1.3×10^{-8} cm/s, 3.7×10^{-8} cm/s, and 6.7×10^{-8} cm/s were determined from the large and small ring infiltrometers, and water-balance data, respectively, during the third year of monitoring.

Geostatistical analysis of flux data measured by the small ring infiltrometers indicated that infiltration flux was unstructured (random) at a scale greater than 1.2 m. Kriged estimates of the annual mean infiltration fluxes of the liner quadrants were almost identical to the geometric mean of the infiltration fluxes. The implication is that spatial variability of the infiltration properties of the liner was random on the scale defined by the locations of the small infiltrometers.

Calculations of the hydraulic properties of the liner were made from 3 years of data on the small and large ring infiltrometer fluxes and water balance, and indicated that the average saturated hydraulic conductivity of the liner was approximately 2.4×10^{-8} cm/s, 8.3×10^{-9}, and 4.4×10^{-8} cm/s, respectively.

Overall tension values in the liner have decreased with time, a trend reflecting the downward movement of water from the overlying pond. After 3 years of monitoring, tension values indicated that the liner is saturated below a depth between 51 and 69 cm; air is still trapped in the pores below a depth of about 33 cm; and the liner is tension saturated below 69 cm. Water collected from the underdrains in the north half of the liner during June through September 1991 was probably the result of temperature effects on soil tension in the liner. Water stopped exiting the liner as temperatures cooled.

An effective diffusion coefficient of 8×10^{-6} cm^2/s was found to describe the tritium concentration profile at 168, 475 and 700 days, after tritium was added to the liner pond.

DISCLAIMER

This report was prepared as an account of work sponsored by the Illinois Hazardous Waste Research and Information Center and the U.S. Environmental Protection Agency, and performed by the Illinois State Geological Survey. HWRIC and USEPA provided peer review; however, ISGS has sole responsibility for conducting the experiment and reporting the results. Mention of trade names or commercial products is for information only and does not constitute endorsement or recommendation for use.

INTRODUCTION

Only limited research on the performance of earthen liners has been conducted at a scale that approaches field use (USEPA 1988). Detailed field-scale experiments of soil liners were conducted by Rogowski (1990) and Elsbury et al. (1990). Rogowski studied the spatial variability of a soil liner's hydraulic properties; Elsbury focused on soil properties, construction equipment, and laboratory testing conditions in building soil liners. (The emphasis of these studies was not on constructing a soil liner with the lowest possible hydraulic conductivity.) The liners constructed during the studies failed to meet the minimum USEPA requirement for hydraulic conductivity; measurements yielded hydraulic conductivities of 5×10^{-7} (Rogowski 1990) and 1×10^{-4} cm/s (Elsbury et al. 1990). Currently used full-scale equipment was not used in one of the studies, and currently recommended liner construction guidelines were not implemented in the other study because guidelines had not yet been established when the liner was constructed. These studies have provided useful information, however, about soil clod size, moisture content, and the size of construction equipment—information currently being used in the construction of liners.

Daniel and Brown (1988) compiled a table of 14 case studies of operational earthen liners constructed throughout the United States and Canada. Only two met the USEPA hydraulic conductivity requirement of 1×10^{-7} cm/s or less. The two successful liners were the Keele Valley Landfill in Ontario (Daniel and Trautwein 1986) and a test liner in California (Chen and Yamamoto 1987). A rigorous quality assurance program was followed during the construction of both liners. Daniel and Brown (1988) suggested five common causes for the failure of liners to meet the hydraulic conductivity criteria: (1) the liners were too thin; (2) they were constructed improperly (i.e., poor material selection and/or inadequate design); (3) inadequate quality assurance was maintained during construction; (4) desiccation and freezing occurred during construction; and (5) chemical constituents in the waste affected the permeability of the soil.

In some studies, laboratory tests indicated that liner materials could be compacted to achieve the required hydraulic conductivity. Increasing evidence shows that laboratory measurements of hydraulic conductivity tend to be lower than the values based on field data (Daniel 1984, Herzog and Morse 1986, USEPA 1988a).

This study attempts to measure hydraulic conductivity under laboratory conditions, although on a large or field scale and with field-type measurements. The results are compared with normal laboratory procedures. Sources of potential error in laboratory tests of hydraulic conductivity, as discussed by Olsen and Daniel (1979), include (1) compaction and water content greater in laboratory samples than in field samples; (2) air trapped in laboratory samples; (3) excessive hydraulic gradients used in the laboratory, thus causing particle migration; and (4) the size of laboratory samples being too small. Other researchers have also been concerned with the issue of confidence in laboratory-derived results of hydraulic conductivity of soils related to size and number of samples (Mason et al. 1957, Anderson and Bouma 1973, Daniel 1981). The importance of hydraulic gradient in laboratory tests of hydraulic conductivity has been investigated by Mitchell and Younger (1967); laboratory tests of hydraulic conductivity have been investigated by Mitchell and Younger (1967), Daniel (1981), Zimmie et al. (1981), Brown and Anderson (1982), Acar and Field (1983), and Foreman (1984). Another long-standing concern has been the difficulty of achieving saturation of samples (Smith and Browning 1942).

Literature reviews and information sources pertaining to construction and evaluation of liners are available in USEPA (1979, 1988a, 1988b, 1990), Ely et al. (1983), Rogowski (1990), Rowe (1990), and Quigley (1990). Krapac et al. (1991) reported on early findings of this study.

Background

Compacted soil liners are widely used to contain leachates and liquid wastes at landfill and waste lagoon facilities. The liner functions as a barrier between the hydrogeologic environment and the wastes by limiting seepage from these waste facilities. The USEPA requires that

2

landfills or lagoons containing hazardous wastes have a double liner system, a leachate collection and leak detection system, and two flexible membrane liners, all underlain by a compacted soil liner. Disposal requirements for municipal refuse are less stringent than those applying to hazardous waste; naturally occurring or recompacted soil materials usually are permitted to be used as the sole liner in municipal landfills. However, more rigorous landfilling requirements for municipal wastes may be adopted by individual states in the near future. The Resource Conservation and Recovery Act (RCRA) requires that the earthen part of the liner must be at least 0.9 m thick and have a saturated hydraulic conductivity of no more than 1×10^{-7} cm/s (USEPA 1987).

In the fall of 1985, the Illinois State Geological Survey began this long term study of a "field-scale" soil liner in cooperation with the USEPA Risk Reduction Engineering Laboratory. The Illinois Hazardous Waste Research and Information Center (HWRIC) joined in supporting this project in 1987. The study has focused on the following goals:
- determine whether the USEPA hydraulic conductivity of 1×10^{-7} cm/s can be achieved;
- determine construction practices and quality control needed to construct a liner that meets requirements;
- determine the transit time of water and tracers through a soil liner;
- quantify the spatial variability in hydraulic conductivity and tracer transport that may be expected in a well constructed soil liner;
- test the accuracy of predictive methods to estimate the transit time of water and tracers through a soil liner.

The study proceeded through several phases. Phase I included an evaluation of soil properties that make soils suitable for use in liners, the characterization of regional soils, and the selection of a soil for use in this project. The results are reported in Krapac et al. (1991).

In the second phase of the project, a prototype liner was constructed to test construction practices and monitoring methods. The results are reported in Albrecht and Cartwright (1989), Albrecht et al. (1989), and Krapac et al. (1991). The prototype study indicated that ISGS construction practices and quality control procedures needed modifications. Information was also obtained on the suitability of various monitoring procedures.

The final phase, which began in October 1987, was the construction of the field-scale experiment, installation of the monitoring system, and collection of long term data on liner performance. This phase has not yet been completed. The initial results of the monitoring program have been reported in Krapac et al. (1990a,b), Cartwright et al. (1990), Krapac et al. (1991), and Panno et al. (1991). The results presented in this report cover more than 3 1/2 years (April 1988 to December 1991) of monitoring the field-scale soil liner.

METHODS
Liner Construction/Instrumentation
The large-scale liner was constructed using common engineering technologies. The emphasis was on compliance with strict specifications for quality control in construction. Information regarding the construction methodology, quality control techniques used during liner construction, and physical properties of the liner are given in detail in Krapac et al. (1991).

Performance of the large-scale liner is assessed in terms of the rates of (1) water infiltration, (2) wetting-front advancement, and (3) tracer migration through the liner. A 31-cm-deep pond overlies the liner. Various instruments, including large and small ring infiltrometers, tensiometers, lysimeters, and evaporation pans, are used to monitor the infiltration and movement of water and tracers through the liner (fig. 1). Krapac et al. (1991) present details on instrument location, construction, and techniques of installation in the liner, and monitoring of the instruments.
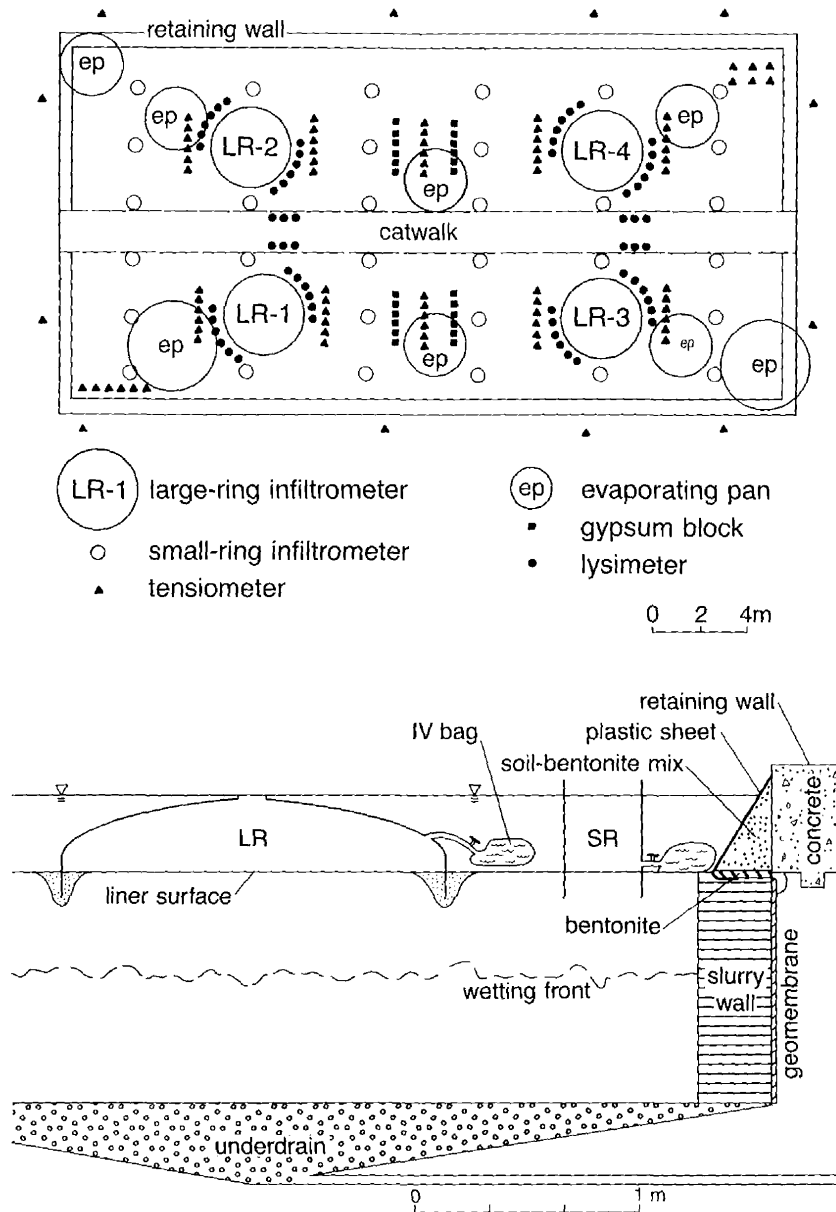
3

Figure 1 (above) Plan view of the full-scale liner experiment shows the instrument layout. (below) Cross-sectional view shows details of construction; the vertical and horizontal scales are the same.

Data Analysis

■ Infiltrometers

Thirty-two small ring (0.3 m in diameter) and four large ring (1.5 m in diameter) infiltrometers were used to measure the infiltration flux of water into the liner. Infiltration flux values were calculated using the cumulative volume of water that infiltrated from each infiltrometer for the monitoring period. For each infiltration ring, cumulative infiltration volumes were plotted with respect to time. The slope of the line for each year of infiltration data was determined using linear regression analysis. The slope of each regression line, divided by the cross-sectional area of each infiltrometer, is the long term average, steady-state infiltration flux.

A water balance technique was used to determine the overall amount of water infiltrating the liner. The water balance was determined by subtracting the volume of water lost from the pond because of evaporation from the total volume of water added to the pond to maintain a near-constant level. The same regression technique used with the infiltrometer data was also used to analyze water balance data. Details of the data analysis can be found in Krapac et al. (1991).

4

■ Tensiometers

The pressure transducer tensiometers consist of a porous ceramic cup connected by nylon tubing to a pressure transducer. Details regarding the theory of operation, construction, installation techniques, and location of the tensiometers can be found in Krapac et al. (1991). The pressure-transducer tensiometers, when connected to a power supply, produce changes in output voltage in response to changes in soil–water tension. The voltage output from each transducer is converted to tension values, as described in Krapac et al. (1991). The initial tension values are adjusted to compensate for the weight of the column of water between the porous cup and the transducer. Based on additional data collected during the second and third years of monitoring and further analysis, it is concluded that the corrections presented in Krapac et al. (1991) are not necessary.

An additional adjustment was made to the tension values to compensate for drift over time in the transducer null-pressure voltage. Null offset is the output voltage that a differential transducer produces when both measurement ports of the transducer are subjected to the same pressure (in this case, atmospheric pressure). In theory, the null offset voltage should be zero. In practice, it is usually shifted to some other number that, when converted to tension, is constant and usually less than the equivalent tension of 10 cm water, although it may be as great as 30 cm water. Transducers that produced large initial null offsets were replaced. Instrument drift was determined by measuring null voltage values periodically, which entailed disconnecting all tensiometers from the transducers for 3 days while the data-logger continued recording output voltages at 10-minute intervals. The average voltage for the third day was used to determine the null offset voltage correction for each individual transducer and to calculate the drift since the last measured null offset voltage. The drift in null offset voltage was assumed to be linear with respect to time to allow the calculation of correct tension data.

The soil tension results presented are based on monthly averages. Because the liner pond was filled on April 12, 1988, averages were calculated from the 12th of each month to the 11th of the following month. For example, the average soil tension for April 1988 was calculated from all soil tensions measured from April 12 to May 11, 1988.

■ Hydraulic Conductivity

Saturated hydraulic conductivity was determined from measurements of steady-state infiltration rate and hydraulic gradient; both Darcy's law and the Green–Ampt equation were used. Darcy's law can be written to calculate hydraulic conductivity as follows:

$$K_{sat} = -\frac{Q}{IA} \tag{1}$$

where Q is discharge, or in this case infiltration rate per unit time, K_{sat} is saturated hydraulic conductivity, I is the hydraulic gradient, and A is the cross-sectional area of the infiltrometer. The ratio Q/A also provides the long term, steady-state infiltration flux. The average infiltration flux in each infiltrometer, for each monitoring year, was used to calculate hydraulic conductivity for each year. The gradient was determined from the soil tension data, which was measured by the pressure transducer tensiometers. The average annual gradient was also used in the calculation of hydraulic conductivity for each monitoring year; the average annual gradients were 1.68, 1.83, and 1.82 for the first, second, and third monitoring years, respectively.

Green and Ampt (1911) modeled the infiltration flux as a function of the total quantity of water that infiltrated the soil. Their equation assumes that the wetting front is sharp, the pressure potential at the front is constant, and the wetted zone is saturated and of constant saturated hydraulic conductivity. This approximation differs from Darcy's law in that the depth of the

5

wetting front is required instead of hydraulic gradient. Incorporating these assumptions, the analytical solution for infiltration flux is an equation that resembles Darcy's law:

$$K_{sat} = i[1 + \frac{h + \psi_f}{L_f}]$$

(2)

where K_{sat} is the saturated hydraulic conductivity, the bracketed term is the hydraulic gradient where h is the ponding depth and ψ_f is the pressure potential at the wetting front, L_f is the depth to the wetting front, and i is the steady-state infiltration flux.

The depth of the pond (h) was 29.5 cm for the first 406 days of ponding and 31.0 cm thereafter. An average height of 30.8 cm was used for pond depth in calculations for the second year, and 31.0 cm was used for the third year. Tensiometer and water-balance data suggested that the wetting front had moved to an average depth of approximately 24, 44, and 61 cm by the end of the first, second, and third year, respectively. The uniform pressure potential ahead of the wetting front was assumed to be the same as the matric potential at the first set of tensiometers below the wetting front; this value was 7 cm of water at the end of 1 year, 6 cm of water at the end of 2 years, and 1 cm of water after 3 years.

Column Experiment

A plexiglass column, 14 cm in diameter and 61 cm long, was constructed to create a sealed microenvironment in which the effects of temperature on pressure potential could be observed (fig. 2). The soil used for this experiment had been collected during construction of the large-scale liner and stored in plastic bags to prevent drying. Prior to compaction, water was added to the soil to approximately the same moisture content as the large-scale liner (11.4%); the sides of the column were roughened with 60 grit sandpaper; and a high-vacuum silicone grease was applied to help form a seal between the soil and plexiglass. The soil was compacted in 20 lifts, each 2.5 cm thick, by using a 5.08-kg compaction hammer. The surface of each lift was scarified to increase the likelihood of proper interlift bonding. The overall bulk density of the compacted soil in the column was 2.02 g/cm^3, which was greater than the average bulk density (1.84 g/cm^3) of the liner.

The air space at the "bottom" of the column was filled with sand. Tensiometers and thermistors were installed in holes drilled through the column wall and soil. Each instrument was installed near the center of the column at distances of about 11.4, 22.8, and 34.2 cm from the "top" of the column. The holes in the soil and PVC of the column were filled with bentonite and epoxy, respectively. The head space at the top of the column was filled with wood blocks to maintain a confining pressure on the soil column. One absolute pressure transducer was installed in the top air space to monitor air pressure. In addition, thermistors and another atmospheric pressure transducer were located outside the column. The tensiometers and thermistors were connected to a data logger, and instrument output was recorded at regular intervals.

Soil temperature inside the column was controlled by wrapping tygon tubing around the outside of the column through which water was pumped. The column and tubing were covered with insulation and a constant temperature water bath was used to control and maintain the water temperature.

Computer Modeling

The last task of this study was to examine the capabilities of existing predictive models of fluid flow and tracer transport through soil liners. Krapac et al. (1991) used several models suggested by the USEPA to model the first year of monitoring data. Difficulties were encountered with the models, especially for tracer transport.

Sealed top

Air

Transducer

Compacted soil

Output to
data logger

Thermister

Tensiometer   Transducer

Thermister

Tensiometer   Transducer

Thermister

Tensiometer   Transducer

Sand

Sealed bottom
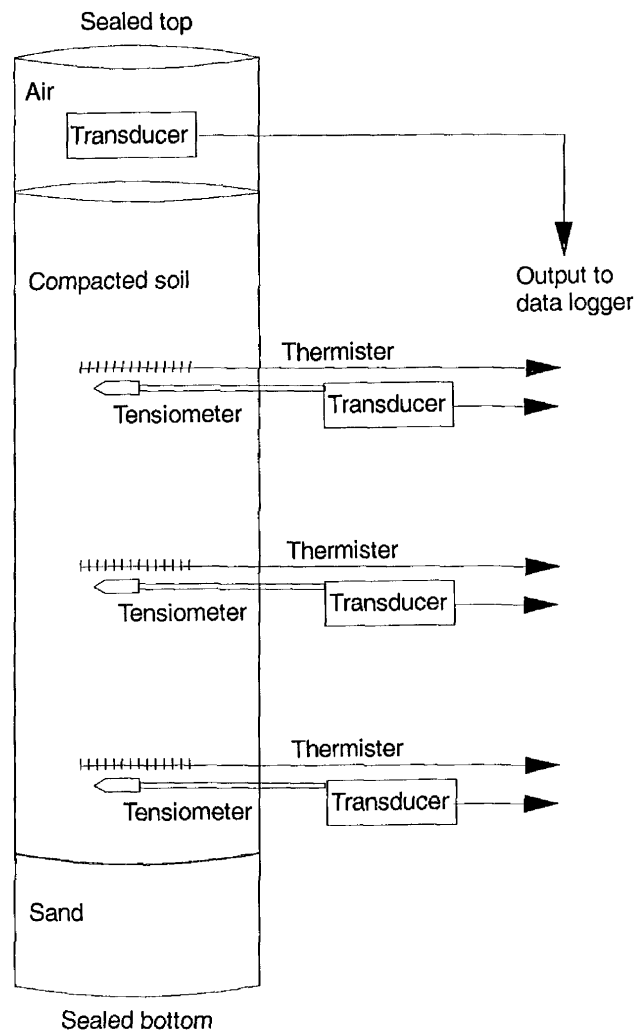
Figure 2 Design of the column experiment.

■ Model Set-up

The EPA code SOILINER (Johnson 1986) was used to predict the movement of water through the large-scale soil liner. Krapac et al. (1991) found that this code produced unsatisfactory results for chemical movement; however, the moisture movement portion of the model appeared to work properly, given the available data. A 2-layer grid consisting of a 91-cm-thick layer, representing the liner, over a 12-cm-thick layer, representing the underlying gravel, was used as the model framework. The upper and lower boundary conditions included a 30-cm, constant head boundry at the top of the liner, representing the pond of water, and a constant negative head at the base of the liner, representing unsaturated gravel. A basal soil layer, as in Krapac et al. (1991), was eliminated. Sensitivity analysis by Krapac et al. (1991) showed that a lower layer below the gravel had little effect on the model results; the lower boundary for this modeling exercise was placed at the base of the gravel layer.

■ Parameter Selection

A moisture characteristic curve, based on three soil samples collected from the apron of the liner outside the ponded area, was developed in the laboratory specifically for this modeling exercise. Soil moisture characteristics curves for each sample for both the wetting and drying cycles were constructed using a pressure cell with a hysteresis attachment. A moisture characteristic curve that incorporated the data from all three liner samples is identified as Soil A
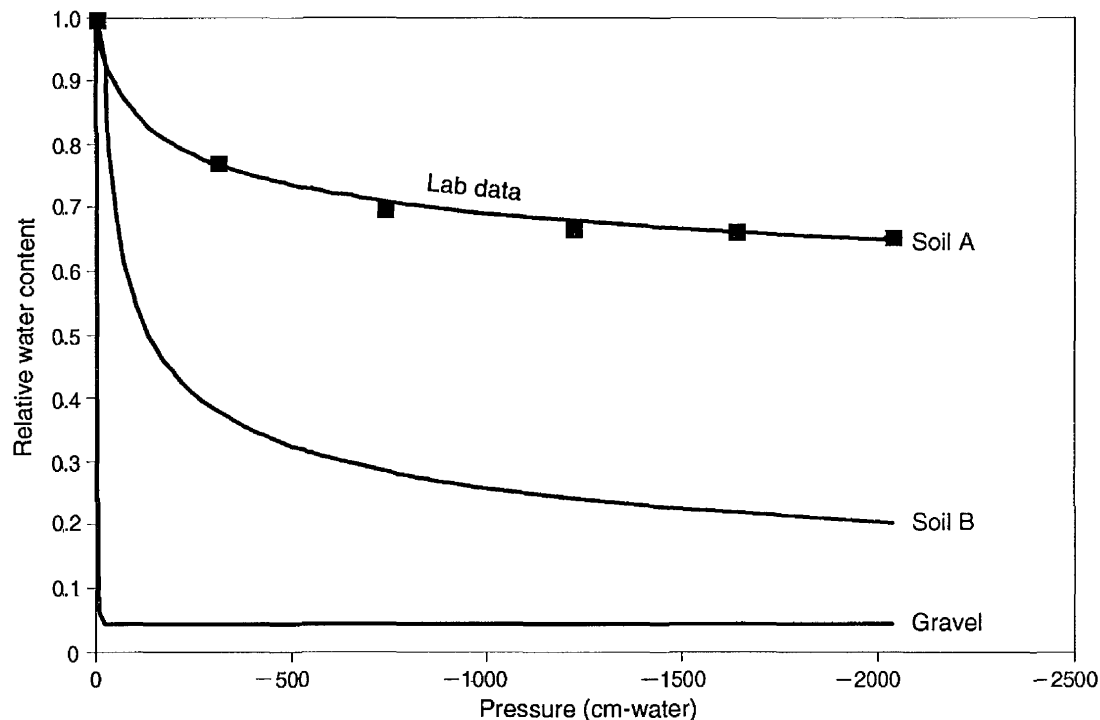
Figure 3 Soil moisture characteristic curves.

in figure 3. The two additional characteristic curves, identified in figure 3 as Soil B and Gravel, are provided by the SOILINER code and represent a hypothetical curve and a curve typical of gravel, respectively. In addition, two other characteristic curves incorporated in the code were used in the model to represent moisture characteristic curves typical of a loamy sand and a heavy clay.

Twenty-three simulations were made to calibrate the model to measured moisture movement and pressure potentials. The saturated hydraulic conductivity used to model the upper portion of the liner was determined from infiltration data collected by the small ring infiltrometers. For some model simulations, different hydraulic conductivity values were assigned to different depths in the liner grid. There were no in situ measurements of hydraulic conductivity at depth in the liner, thus the values were assigned during the calibration of the model and represent attempts to make the model more closely represent the moisture movement and pressure potentials observed in the liner. Four hydraulic conductivity scenarios were modeled (table 1a). One assumed a constant hydraulic conductivity for the entire liner, representative of uniform flow conditions. Two other scenarios assumed a gradual decrease in conductivity with depth in the liner, thus representing changes that could have resulted from additional compaction in the lower soil layers of the liner as the overlying soil layers were added during liner construction. The final scenario assumed an abrupt change in conductivity, which could have resulted from a sudden change from saturated to tension-saturated flow. Two different sets of initial conditions were modeled for pressure potential and moisture distribution in the liner. The first condition assumed a uniform pressure potential distribution throughout the liner, whereas the second was based on tensions measured in the liner before filling of the pond (table 1b).

RESULTS AND DISCUSSION
Infiltration Fluxes
Small and large ring infiltrometers and a water balance were used to measure the infiltration flux of pond water into the liner material. Infiltration flux data collected over the course of 3 years were used, in conjunction with measurements of wetting front and pressure potential, to

determine the saturated hydraulic conductivity of the liner and its areal distribution, and to estimate the transit time of water through the liner.

■ Water Balance Analysis

Water infiltration fluxes for the entire liner were determined using the data collected from the evaporation pans and water flow meter. Figure 4 shows the cumulative water that infiltrated into the liner for the period from April 12, 1988, to July 30, 1991. Two different methods were used to determine infiltration fluxes for each year (labeled as year 1-4 in table 2). In addition, fluxes were calculated for a 3-year period and the entire 3½-year monitoring period. The first method used linear regression to statistically fit a straight line through the data; the slope of the line (volume of water infiltrated/time) was then divided by the area of infiltration to determine an "average" infiltration flux for the time period. The second method used the total volume of water that infiltrated into the liner for the time period divided by the area of infiltration to produce an average infiltration flux. Both methods of data analysis produced similar results; flux values ranging between 9.2×10^{-8} and 5.5×10^{-8} cm/s.

Table 1. Model input parameters.

(a) Model input conditions, hydraulic conductivity, and tension values used to model water movement in the large-scale liner.

I	For model simulations 1 through 4, 13, 16, and 18 a uniform value for hydraulic conductivity was used.
II	For model simulations 5 through 12, 12, 14, 15, 20, and 21 an abrupt change in hydraulic conductivity from 4×10^{-7} cm/s to 4×10^{-8} cm/s was modeled. The depth in which the change in conductivity was made is listed in the table.
III	For model simulations 21 through 23 the hydraulic conductivity was varied at three depths with the change in conductivity ranging from 4×10^{-7} cm/s to 4×10^{-9} cm/s.
IV	For model simulations 17 and 19, the hydraulic conductivity was incrementally decreased from 4×10^{-8} cm/s to 4×10^{-9} cm/s as shown below.

Depth (cm)	Hydraulic conductivity (cm/s)
00–15	4.0×10^{-8}
16–30	2.5×10^{-8}
31–45	1.6×10^{-8}
46–60	1.0×10^{-8}
61–75	6.3×10^{-9}
76–91	4.0×10^{-9}

(b) Initial tension was modeled as either uniform with respect to depth in the liner, or variable with depth. Tensions based on measurements made at various depths in the liner before filling of the pond are shown below.

Depth (cm)	Pressure potential (cm)
00–14	30
15–35	45
36–45	60
46–50	80
51–61	100
62–91	75

Table 2. Infiltration fluxes (cm/s) for the entire liner based on a water balance analysis.

| | | Fluxes determined by | |
| | | Regression analysis | Cumulative infiltration analysis |
Analysis period			
1st year	4/12/88 to 4/11/89	7.8×10^{-8}	9.2×10^{-8}
2nd year	4/12/89 to 4/10/90	6.7×10^{-8}	7.5×10^{-8}
3rd year	4/11/90 to 4/10/91	6.7×10^{-8}	6.6×10^{-8}
4th year	4/11/91 to 7/30/91	5.5×10^{-8}	5.8×10^{-8}
All 3.5 years	4/12/88 to 4/10/91	7.9×10^{-8}	7.8×10^{-8}
All 4 years	4/12/88 to 7/30/91	7.8×10^{-8}	7.6×10^{-8}

Table 3. Geometric mean, log mean, and standard deviation of infiltration fluxes from large-ring and small-ring infiltrometers.

Infiltrometer	Analysis period	Geometric mean flux (cm/s)	Log mean of flux	Standard deviation*
Large ring	1st year	5.7×10^{-9}	-8.243	0.363
Large ring	3rd year	1.3×10^{-8}	-7.878	0.104
Small ring	1st year	8.3×10^{-8}	-7.082	0.135
Small ring	2nd year	6.4×10^{-8}	-7.193	0.178
Small ring	3rd year	3.7×10^{-8}	-7.434	0.250

* The log mean plus or minus 2 times the log standard deviations corresponds to infiltration flux values ranging from 1.07×10^{-9} to 1.46×10^{-7} cm/s for all the data.
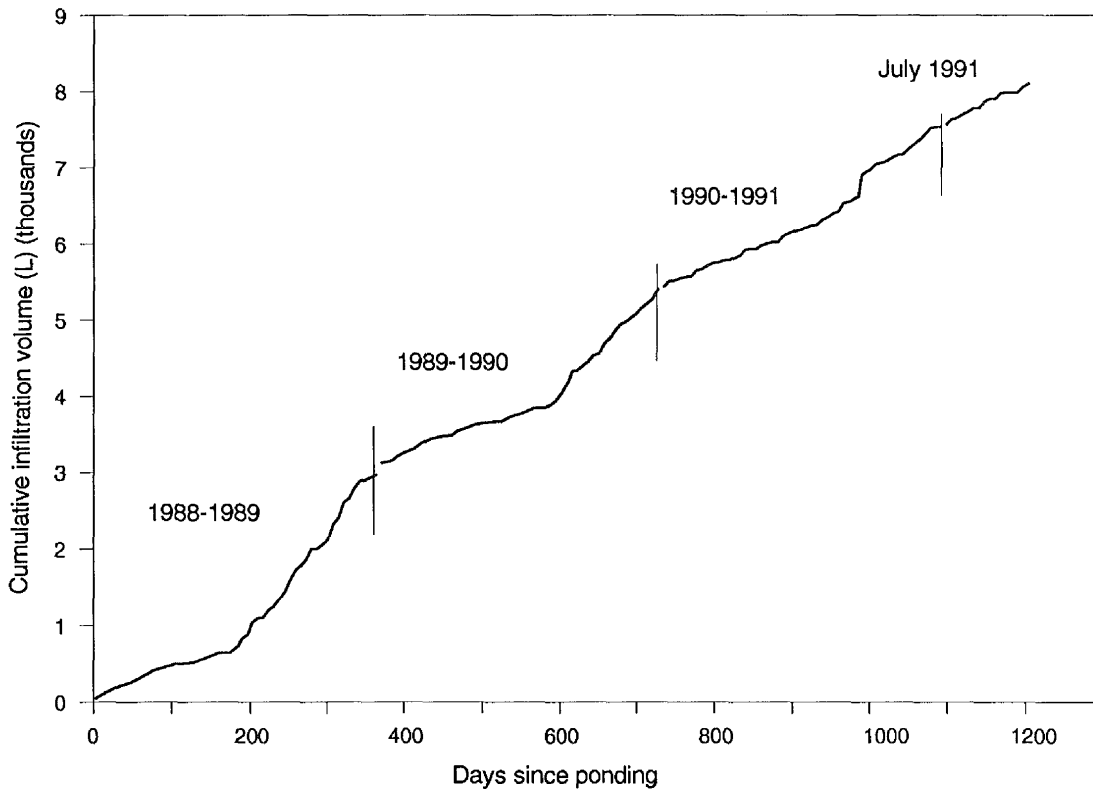
Figure 4 Volume (in liters) of water infiltration into the liner, as determined from water balance data.
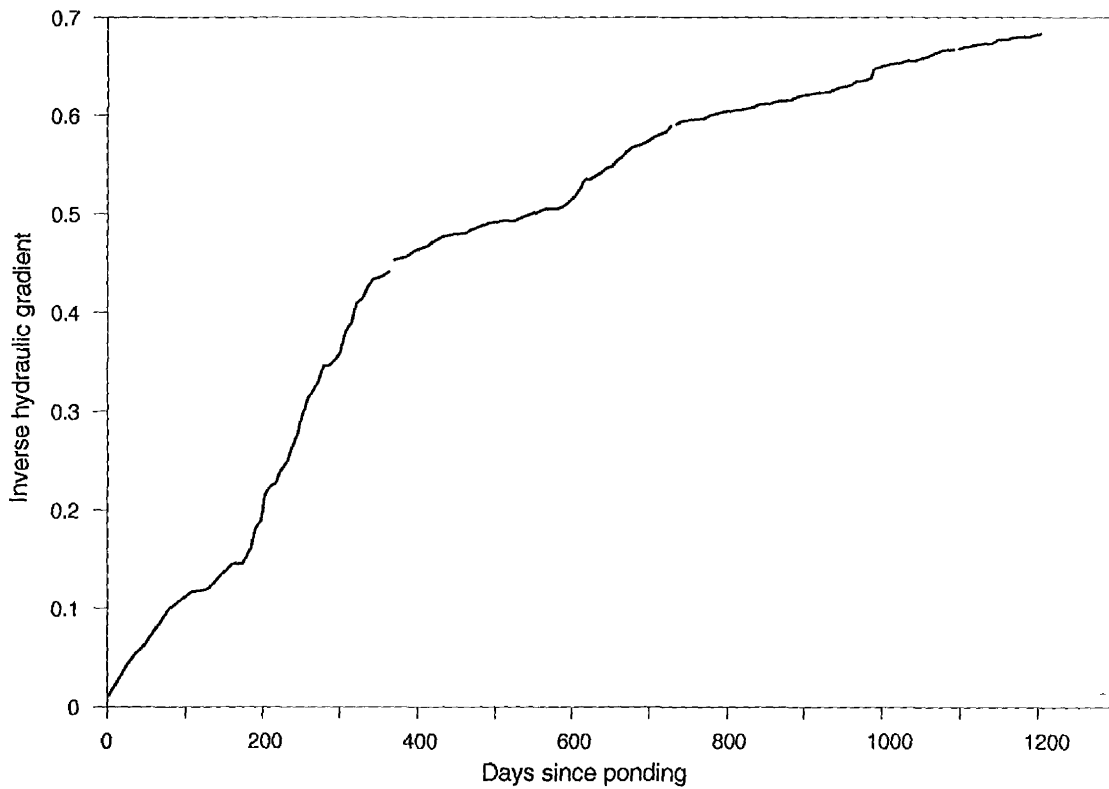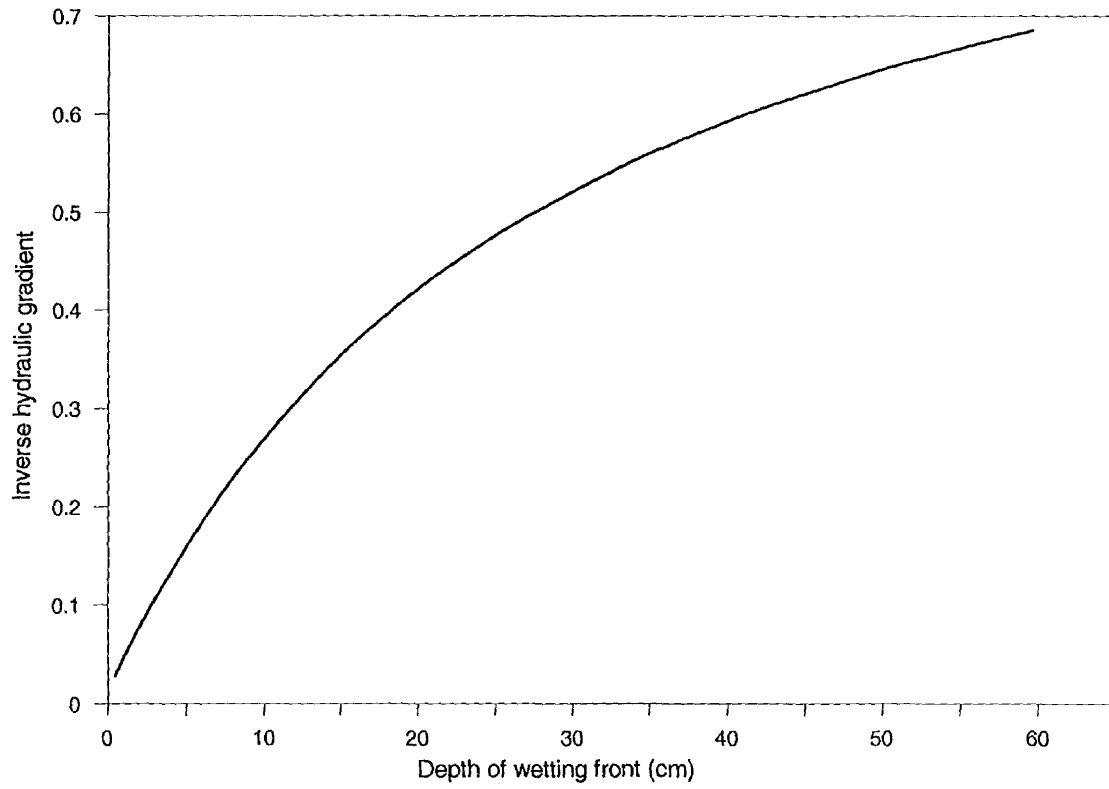
Figure 5 (above) Theoretical curve representing inverse hydraulic gradient as a function of wetting front advancement in the liner. (below) Inverse hydraulic gradient calculated from the infiltration flux data measured for the liner water balance.
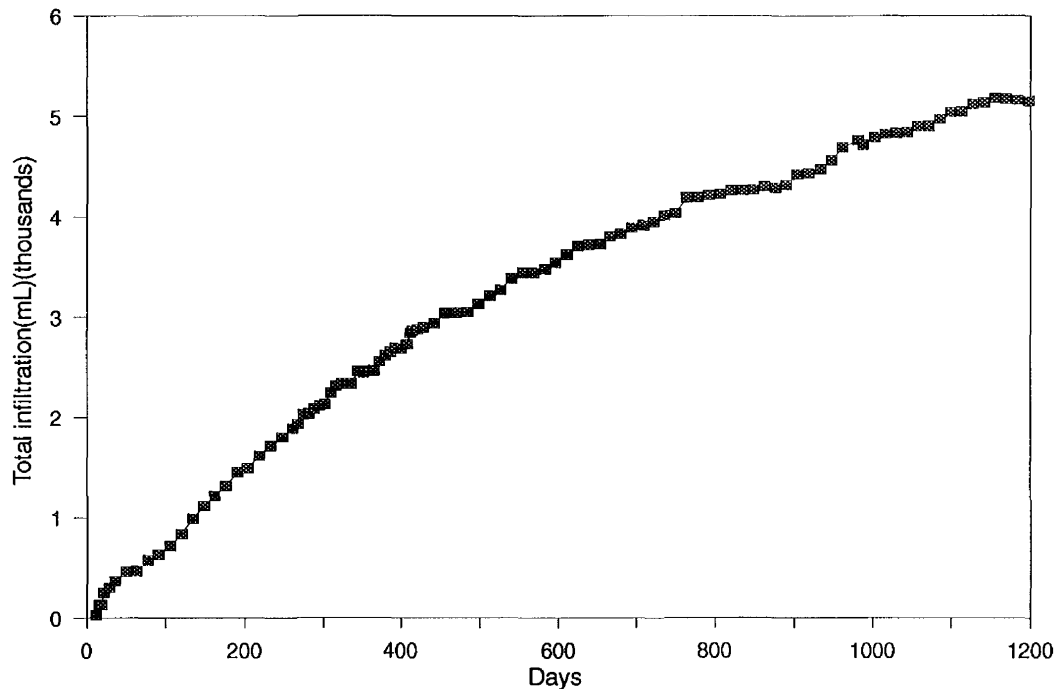
Figure 6 Representative cumulative infiltration curve from small ring 6 of infiltrometer 19.

■ Small and Large Ring Infiltrometers

Curves depicting the change in cumulative infiltration flux with respect to time (fig. 6), as measured by the small ring infiltrometers, appear to have the same shape as a theoretical curve representing changes in the inverse hydraulic gradient as a function of wetting front advancement (i.e. time). That is, the flux data produced curves similar to those that would be expected from a decrease in hydraulic gradient as water infiltrates and the wetting front advances into the liner and the head loss occurs over greater lengths (fig. 5).

Infiltration curves are generally arcuate and occasionally sharply angular, but all show a decrease in flux with time (fig. 6). At the end of the first, second, and third years of monitoring, the geometric mean infiltration fluxes measured by the small ring infiltrometers were 8.3×10^{-8}, 6.4×10^{-8}, and 3.7×10^{-8} cm/s, respectively (table 3). The decrease in infiltration flux with time is expected as the liner approaches steady flow. The infiltration flux at the time of breakthrough (i.e., when the gradient is 1.34) should be approximately 3.4×10^{-8} cm/s using Darcy's law or 3.3×10^{-8} cm/s using the Green–Ampt equation. The latter calculation assumes a pressure potential of zero at the base of liner.

The data representing steady-state infiltration measured by the small and large ring infiltrometers formed two statistically distinct populations during the first year of monitoring (fig. 7) (Panno et al. 1991). Fluxes measured by the large ring infiltrometers were approximately one order of magnitude lower than fluxes measured by either the small ring infiltrometers or the water balance technique. The distribution on the left side of the diagram represents data collected by the small ring infiltrometers. The small ring data are log-normally distributed at the 95% confidence level on the basis of the Kolmogorov–Smirnov test (Benjamin and Cornell 1970).

The second year of monitoring was a transition period for the large ring infiltrometers. Gasses entrapped during compaction and/or biotically generated in the soil below the infiltrometers were degassing from the soil into the water and infiltrometers. Analysis of gas collected from the infiltrometers indicated concentrations in the order of $N_2 > H_2S > CH_4 > O_2 > CO_2$. This combination suggests biotic formation of the gas. The gas escaping from the soil and collecting in the infiltrometer affected the functioning of the infiltrometer, and thus its capability to make
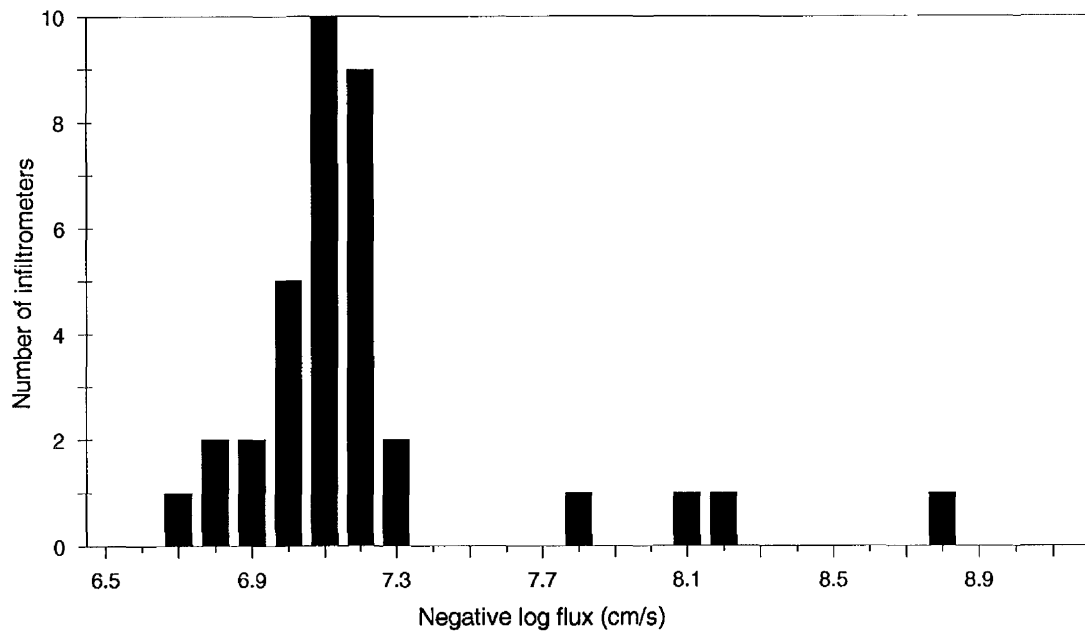
12

Figure 7 Frequency distribution of infiltration fluxes during the first monitoring year for the ring infiltrometers. Four large ring infiltrometers appear on the far right.
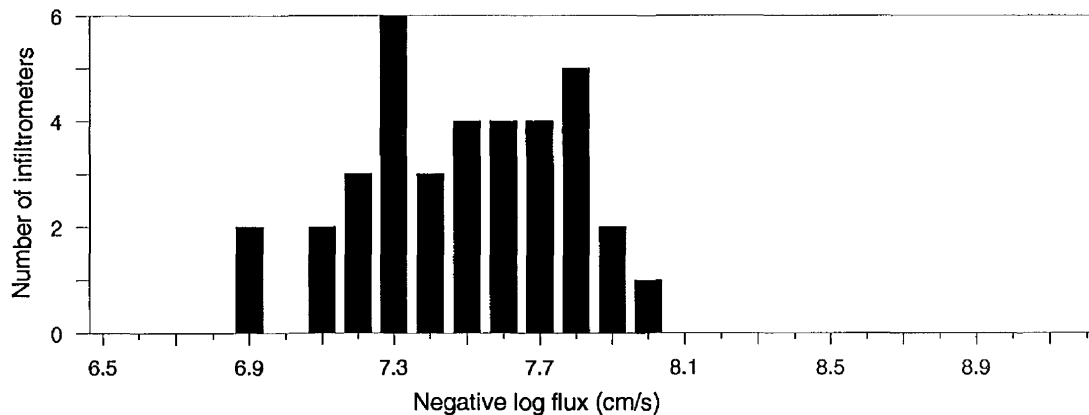
Figure 8 Frequency distribution of infiltration fluxes during the third monitoring year for ring infiltrometers.

measurements; the result was an apparent decrease in flux. Gases trapped in soil pores caused physical changes that reduced fluxes in the liner. Belanger and Mikutel (1985) found that sealing seepage meters (analogous to ring infiltrometers) from the atmosphere in a field experiment resulted in the occurrence of anaerobic conditions in the seepage meters; whereas seepage meters that were allowed direct contact with the atmosphere remained aerobic.

It has been shown that methane gas trapped within materials of low hydraulic conductivity (specifically peat) reduced the hydraulic conductivity of that material (Brown et al. 1989). The reduction in flux in the large infiltrometers indicates a lower hydraulic conductivity, which is mainly attributed to gas blocking the pore spaces within the material.

A simple correction of the infiltration data measured in the large infiltrometers could be used to account for gas accumulation in the infiltrometers; however, inconsistency in the presence and amount of gas generated within each infiltrometer made the use of a correction somewhat tenuous. Gas was generated in infiltrometers 3 and 4, and after repeated removal of the gas, the fluxes in these two infiltrometers increased to values comparable to those of the small ring infiltrometers. This occurrence suggests that a simple correction of these data would be

13

Table 4. Comparison between the third-year infiltration flux values relative to the flux values for the summation of the period from day 50 to day 550.

Large ring infiltrometer number	Third year data regression analysis	Day 50 to 550 data summation method of analysis
1	1.06×10^{-8}	8.2×10^{-9}
2	1.52×10^{-8}	2.0×10^{-8}
3	1.14×10^{-8}	1.7×10^{-8}
4	1.42×10^{-8}	1.0×10^{-8}

sufficient. In contrast, infiltrometer 2 also had a gas build-up, yet never showed a decrease in infiltration flux prior to purging of the gas or an increase flux after purging; the use of a correction for the data set seems questionable. In the case of infiltrometer 1, no gas build-up was ever identified. Because of the inconsistency of gas release within the infiltrometers and the necessity for comparison of fluxes between infiltrometers, no correction was made to the large ring infiltrometer fluxes. Gas was periodically purged from the infiltrometers until gas generation ceased in the liner soil in the fall of 1986. After cessation of gas generation, the flux measurements from the large ring infiltrometers became similiar to the estimates for both the small ring and water balance infiltration fluxes.

Because of the effect of the gas on infiltration, it was not possible to use the regression method to calculate a representative infiltration flux from the large ring infiltrometers for the two monitoring years. However, by using the total water loss from each large ring infiltrometer summed for the period between 50 and 550 days after ponding (after significant matric suction effects on infiltration ceased and after gas was regularly purged from the rings), it was possible to calculate fluxes comparable to those calculated for year 3 (table 4). The mean flux for the large ring infiltrometers during the third year, calculated by using the regression technique or by summing the water loss, was 1.3×10^{-8} cm/s and 1.4×10^{-8} cm/s, respectively.

The third year distribution of the infiltration fluxes for the small and large ring infiltrometers is an almost asymmetrical log-normal distribution (fig. 8). The two outliers on the left in figure 8 are fluxes measured in small ring infiltrometers 1 and 3 in the northeast quadrant of the liner. The north half of the liner, and especially the northeast quadrant, experienced what initially appeared to be breakthrough in the summer of 1992. Higher flux values in this quadrant are consistent with early (albeit short-lived) "leakage" in this quadrant (see section on transit time).

■ Spatial Variability

Geostatistical analysis was conducted using log-transformed, infiltration flux data measured by the small ring infiltrometers during the first, second, and third years of monitoring, and by the small and large ring infiltrometers during the third year of monitoring. The methodology used in the geostatistical analysis of the infiltration flux data may be found in Panno et al. (1991). The analyses were conducted to estimate the spatial average of the infiltration flux for the entire liner and each of its quadrants. A structural analysis that was performed (following Journel and Huijbregts 1978) consisted of the construction and interpretation of sample variograms, and the selection of a model variogram to best fit the structure of the log-transformed infiltration flux data. The model variogram was used in the kriging analysis to determine the mean infiltration flux values.

A sample variogram is a measure of the average spatial variability in the data as a function of the distance between datum points. If the sample variogram is a horizontal line with a value equal to the sample variance, the data are considered random in space (unstructured at the scale of measurement) and classical statistics can be used. If the data are structured, the variogram will show a relationship for the distance between datum points and how well adjacent
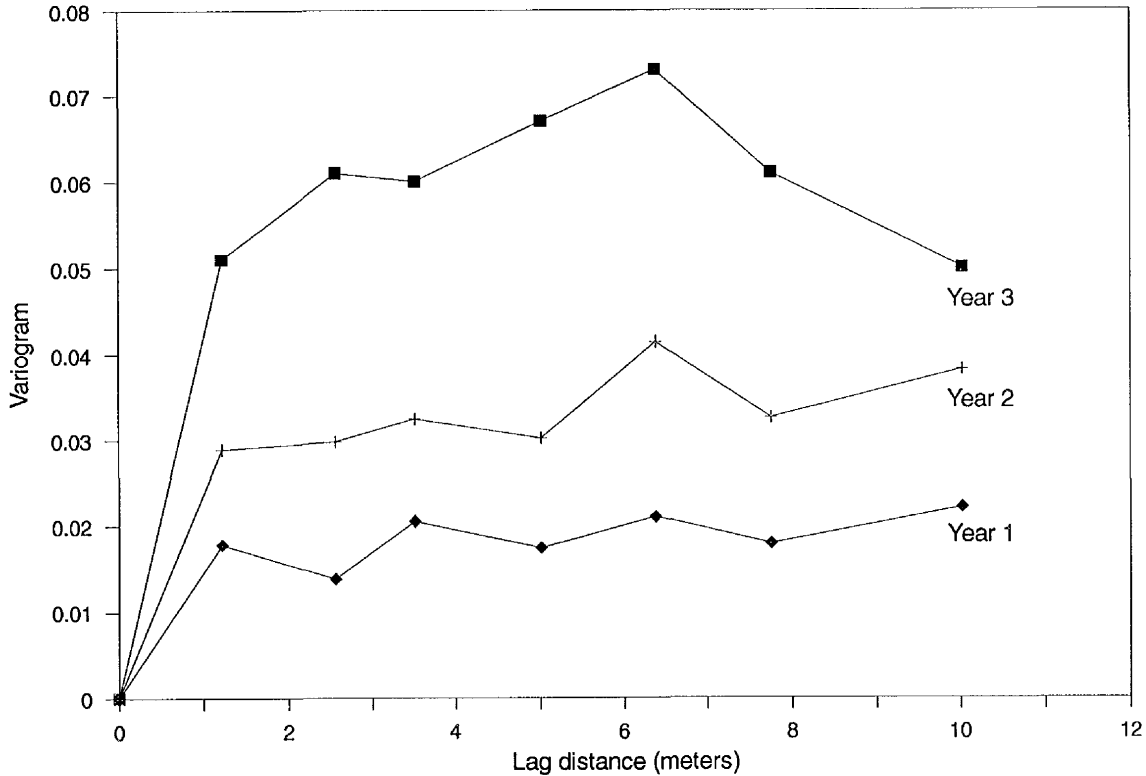
Figure 9 Variograms of infiltration fluxes measured during the first, second, and third year of monitoring by the small ring infiltrometers.

datum points correlate with one another. For an isotropic variogram, data variability is the same in all directions. If the data variability is a function of direction, the data are considered statistically anisotropic and the use of more advanced techniques (e.g., kriging) is necessary to estimate the mean.

A structural analysis of the small ring infiltration data (Panno et al. 1991) could not distinguish between isotropic and directional variograms, thereby indicating no evidence for anisotropic conditions. As a result, only the isotropic variogram was considered. The sample isotropic variograms of the log infiltration flux for the first, second, and third year data are presented in figure 9. As noted above, the degree of variability increases from the first to third monitoring years.

The variogram for each year is nearly flat, indicating a largely unstructured medium. At the first separation distance of about 1.2 m, the variogram for years 1 and 2 has a value essentially equal to the variance (0.019 for year 1 and 0.033 for year 2). The variogram fluctuates about the variance for separation distances beyond 1.2 m. It is possible to interpret the slope of the variogram for year 3 as an indication of structure; however, if an exponential variogram is assumed with a sill value equal to the variance, the correlation scale (defined as the lag distance where the variogram attained 63% of its sill value) is less than 1.2 m. Again, the data indicate the infiltration flux is unstructured at the scale of the smallest separation distance.

For several reasons, an exponential model was assumed to fit the variogram instead of a linear model that incorporated a nugget effect. Linear models assume a nonfinite, à priori variance; whereas the exponential model assumes a finite variance equal to the sill value. The data in figure 9 indicated that the sill of the experimental variograms is nearly identical to the variance of the data. Although the variogram appears to have a slope that would suggest a linear model

Table 5. Calculated and estimated mean fluxes (cm/s) in each quadrant of the liner using data from the small-ring infiltrometers.

Quadrant	1st year		2nd year		3rd year	
	Geometric mean flux	Kriged estimated flux	Geometric mean flux	Kriged estimated flux	Geometric mean flux	Kriged estimated flux
Northeast	9.95×10^{-8}	9.90×10^{-8}	8.04×10^{-8}	8.00×10^{-8}	5.30×10^{-8}	5.30×10^{-8}
Southeast	7.34×10^{-8}	7.30×10^{-8}	6.12×10^{-8}	6.10×10^{-8}	2.82×10^{-8}	2.80×10^{-8}
Northwest	7.98×10^{-8}	7.90×10^{-8}	6.25×10^{-8}	6.30×10^{-8}	3.16×10^{-8}	3.10×10^{-8}
Southwest	8.04×10^{-8}	7.90×10^{-8}	5.48×10^{-8}	5.50×10^{-8}	3.90×10^{-8}	3.80×10^{-8}
All	8.28×10^{-8}	8.30×10^{-8}	6.41×10^{-8}	6.40×10^{-8}	3.68×10^{-8}	3.70×10^{-8}

be used, 95% confidence limits for the variogram were calculated using a Jacknife procedure (Shafer and Varljen 1990). The varigram data points were within the confidence limits in all cases, suggesting that the apparent slope is not statistically significant. The use of a large nugget in a model would incorrectly suggest that the experimental error associated with measurement of the water infiltration is much larger than the natural variability. The use of a variogram model with a sill and a small or zero nugget appears to be a more physically representative of the hydrologic processes occurring in the liner than the use of a linear model.

The mean infiltration flux for the entire liner and for each quadrant was estimated by (1) the geometric mean of the measurements made within each quadrant, and (2) kriging, using an isotropic variogram model (Journel and Huijbregts 1978). The USEPA geostatistical analysis package, GEO–EAS (Englund and Sparks 1988), was used to produce the kriged average infiltration flux. Only those data within the quadrant were used for quadrant estimates. The geometric and kriged means for each quadrant were similar to one another, and the mean infiltration fluxes of the four quadrants were approximately the same over the entire liner (table 5). The geometric mean and kriged estimate of the mean infiltration flux for the entire liner were essentially the same (table 5).

The statistical analyses suggest that the infiltration flux of the liner was unstructured at a scale greater than 1.2 m. The unstructured nature of the infiltration flux was supported by the similarity between the mean infiltration flux estimates from the geometric mean and kriging. In terms of the properties of the liner, the statistical analysis confirmed that it is possible to construct a uniform liner. In addition, classical statistics should be adequate for the estimation of the mean infiltration flux of the liner and the uncertainty associated with that estimate.

■ Optimal Sample Spacing

A variety of designs for developing sampling schemes has been proposed. A basic step of any sampling scheme is to determine the number of samples to be collected and analyzed. A classical statistical approach was used to determine the number of infiltrometers (samples) necessary to estimate the average infiltration flux (saturated hydraulic conductivity) of a liner or test pad. Sample size estimates were made using log-transformed fluxes measured by the large and small ring infiltrometers. Sample sizes are presented for various levels of precision in estimating the population mean flux at a given confidence level.

The central limit theorem of probability theory allows that, given a sample mean and variance, confidence intervals may be constructed for the true mean of the population. The confidence interval is determined by

$$CI = \bar{x} \pm \frac{s}{\sqrt{n}} t_{(\frac{\alpha}{2}, n-1)}$$ (3)

The confidence interval can be used to estimate the number of samples (n) necessary to achieve a sample mean within a given error level (r) of the population mean at a level of confidence (1-α). If

$$\bar{X} \pm \frac{s}{\sqrt{n}} t_{(\frac{\alpha}{2}, n-1)} = \bar{X} \pm r\bar{X} \tag{4}$$

then solving for n:

$$n = [t_{(\frac{\alpha}{2}, n-1)} \times \frac{s}{r\bar{X}}]^2 \tag{5}$$

Equation 5 must be solved by iteration because of the degrees of freedom (n-1) used to determine the t statistic change in response to the sample size. By setting the value of t constant (for these sample size determinations t=2), it is possible to calculate the sample size required to estimate the population mean within a precision and confidence level. The selection of t equal to 2 was thought to be a reasonable assumption on the basis that, at degrees of freedom greater than 29 (n>30), the t statistic is for all practical purposes the same as the normal distribution, where t=Z=1.96 when α/2= 0.025. This assumption was thought to be reasonable as a first approximation of the number of infiltrometers to use to determine the average saturated hydraulic conductivity of a liner. It must be cautioned that the use of these estimated sample sizes for other liner systems assumes that the liner will have variabilty similar to this experimental liner. Because of differences in construction techniques, scale of construction equipment, and size of liner, the variabilty of commercial-scale liners may be different from the large-scale experimental liner used in this study. These estimates could be used as a first approximation in determination of the number of infiltrometers to use in the first phase of a multiphase sampling plan.

Estimates of sample sizes were made on the basis of mean and standard deviations of fluxes measured by the large and small ring infiltrometers for the first, second, and third years of monitoring the liner. In addition, fluxes measured during the second year of monitoring by the small ring infiltrometers were analyzed by block kriging, which made it possible to estimate infiltration fluxes for areas the approximate size of the large ring infiltrometers (table 6).

Results of this approach in estimating the number of infiltrometers necessary to monitor a liner at a given level of precision and confidence indicate that to obtain precision levels of less than 5% requires only one randomly placed infiltrometer. For precision levels higher than 5%, an impractically high number of infiltrometers would be required. Estimates of infiltration fluxes by the ring infiltrometer method can, at best, estimate the average infiltration flux of the entire liner to within ±10% at a 95% confidence level.

Table 6. Number of infiltrometers required to attain a sample mean infiltration flux within ± 1%, 5%, 10%, and 25% of the population mean at a 95% level of confidence.

Precision level (%)	Sample sizes based on first year of monitoring		Sample sizes based on second year of monitoring			Sample sizes based on third year of monitoring	
	Large-ring infiltrometers	Small-ring Infiltrometers	Large-ring Infiltrometers	Small-ring Infiltrometers	Kriged	Large-ring Infiltrometers	Small-ring Infiltrometers
1	78	15	114	24	12	3	45
5	3	1	5	1	1	1	2
10	1	1	1	1	1	1	1
25	1	1	1	1	1	1	1
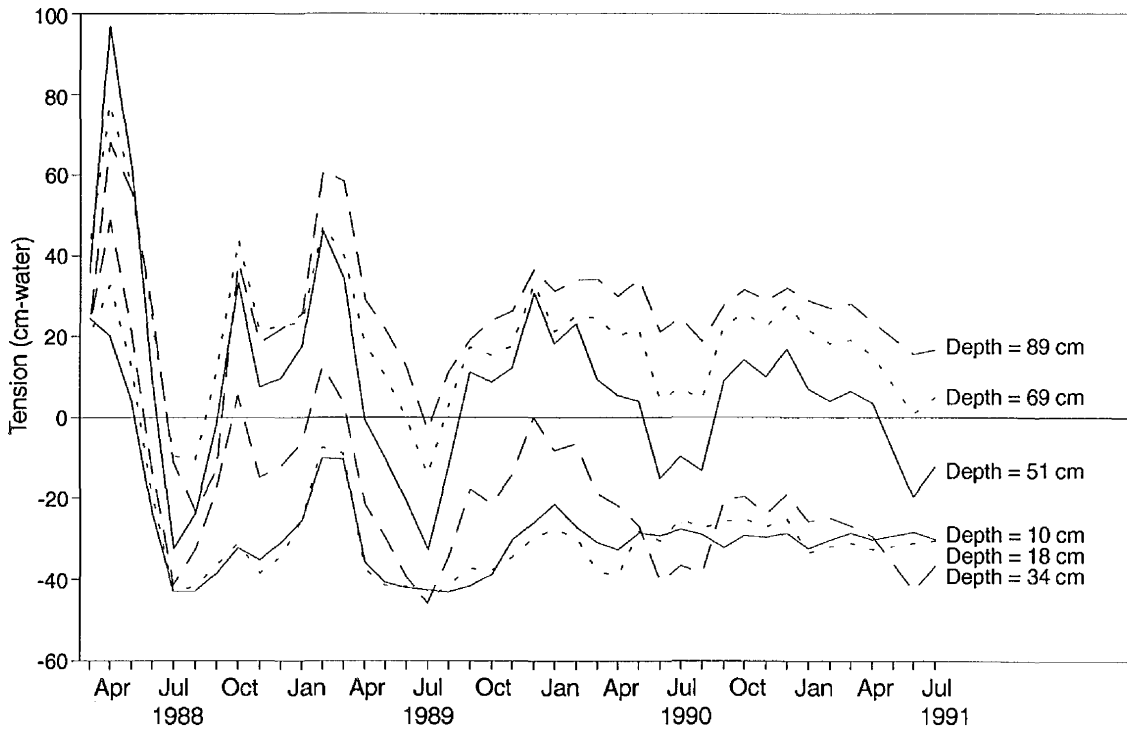
Figure 10 Average monthly tension relative to time at six depths in the liner.

■ Soil–Water Tensions

Tension, or pressure potential, is a measure of the energy status of soil water, as measured in centimeters of water. Therefore, a saturated soil will have a negative tension value and an unsaturated soil will have a positive tension value. Soils can and commonly do, however, have positive tension values indicative of unsaturated conditions, under which all pore spaces are saturated. This situation occurs near the water table in the tension-saturated zone. The thickness of the tension-saturated zone is partly dependent upon the grain size of the soil, and it may be as much as 200 cm in fine grained soils (Lohman 1972).

Tension in the soil liner has been monitored since 30 days before ponding. Ideally, these data may be used to monitor the downward movement of moisture and the wetting front; however, the soil tensions in the large-scale liner have been highly variable. This variability prompted a secondary investigation into the effects of pressure and temperature changes on tension. The tension data, when combined with instrument elevation data, can also be used to determine head, which is then used to calculate the hydraulic gradient within the liner. Hydraulic gradient is needed to calculate hydraulic conductivity from flux values.

Figure 10 shows changes in the average monthly tension with respect to time for each layer of tensiometers. A layer corresponds to the set of instruments installed at a given depth in the liner. Layers 1, 2, 3, 4, 5, and 6 correspond to instrument depths of 10, 18, 33, 51, 69, and 89 cm, respectively. Tension values, which were highest early in 1988, indicate the unsaturated conditions in the liner prior to filling of the pond. Three months after the pond was filled, the tensiometers at depths of less than 33 cm (layers 1–3) were measuring tensions indicative of saturated conditions. Since then, tensions at depths of less than 18 cm have remained fairly constant at values indicating saturation. The tensiometers at a depth of 33 cm have consistently measured negative tensions (saturated conditions) since 1 year after liner monitoring was initiated. Tension at depths greater than 51 cm has been decreasing with respect to time, but tension values have generally been positive even after 3 years of monitoring, thus indicating unsaturated conditions. Seasonal fluctuations in tensions have been observed by tensiometers
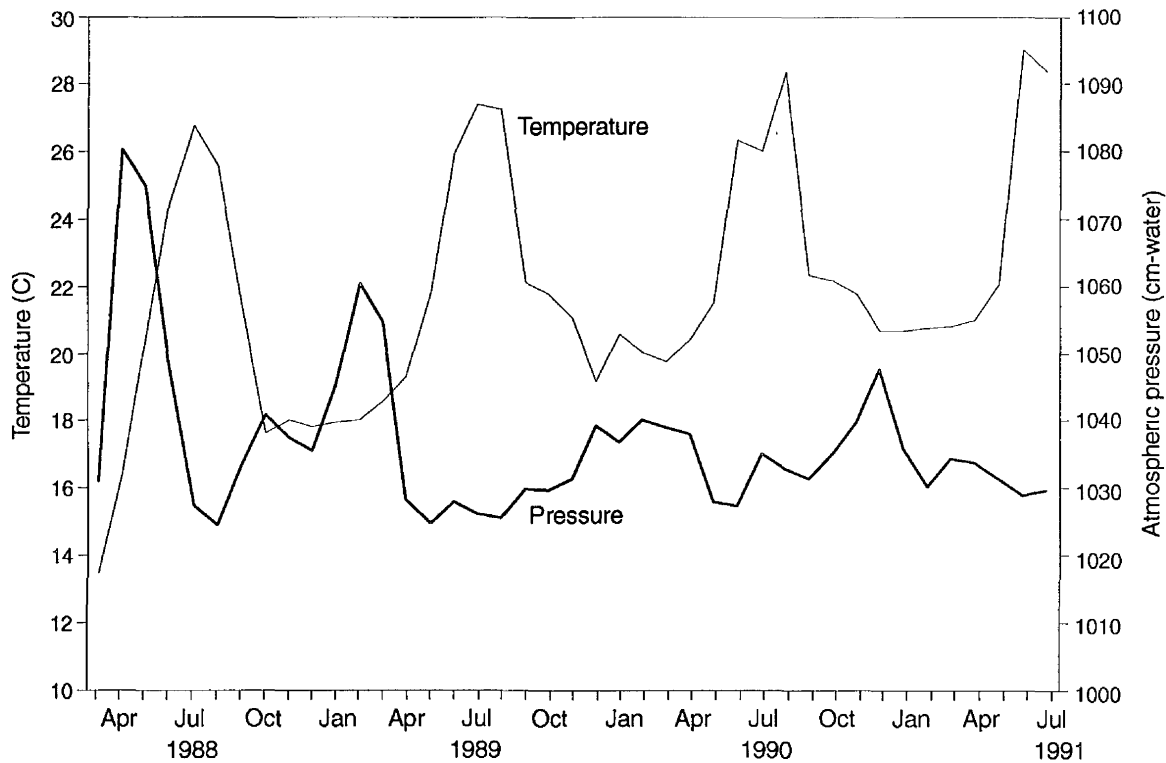
Figure 11 Average monthly temperature and atmospheric pressure in the liner shelter.

located at depths equal to or greater than 33 cm (fig. 10). Changes in tensions at depths of 10 and 18 cm in the liner stopped showing seasonal fluctuations approximately 2 years after liner monitoring began.

Figure 11 shows monthly averages of atmospheric pressure and temperature recorded in the shelter housing the large-scale liner. Pressure and temperature fluctuations show seasonal trends similar to those seen in soil–water tensions measured in the liner (fig. 10). Peck (1960a), Norum and Luthin (1968), and Turk (1975) have all suggested that pressure increases will cause entrapped air to occupy less space in the soil, and pressure decreases will cause entrapped air to expand and occupy more space. Thus a decrease in air volume, caused by an increase in atmospheric pressure, would result in an increase in tension and vice versa. Turk (1975) suggested that this effect would be most apparent in fine grained materials, such as those in the liner.

The spatial distribution of tension in the liner is shown in figure 12. Tension values indicated, after 3 years of monitoring, that the liner was saturated from the surface to approximately 33 cm. About one-third of the liner had saturated conditions to a depth of 51 cm; below that depth the liner was generally unsaturated. Tension values were lowest in the northwest quadrant and on the north side of the liner, conditions indicating that greater infiltration had occurred in those areas, as compared to the rest of the liner. The portion of the liner that is saturated after 3.5 years of monitoring is the upper 20 to 33 cm. The lack of tension fluctuation in response to temperature–pressure changes in these layers indicated that there was no entrapped air after the second year of monitoring (fig. 12). Fluctuations in tension beneath this depth indicated the continued presence of entrapped air.

■ Temperature Effects on Tension

A soil column, compacted to simulate conditions in the large-scale liner, was constructed to examine the soil–water tension and temperature relationship observed in the liner. Figure 13

19
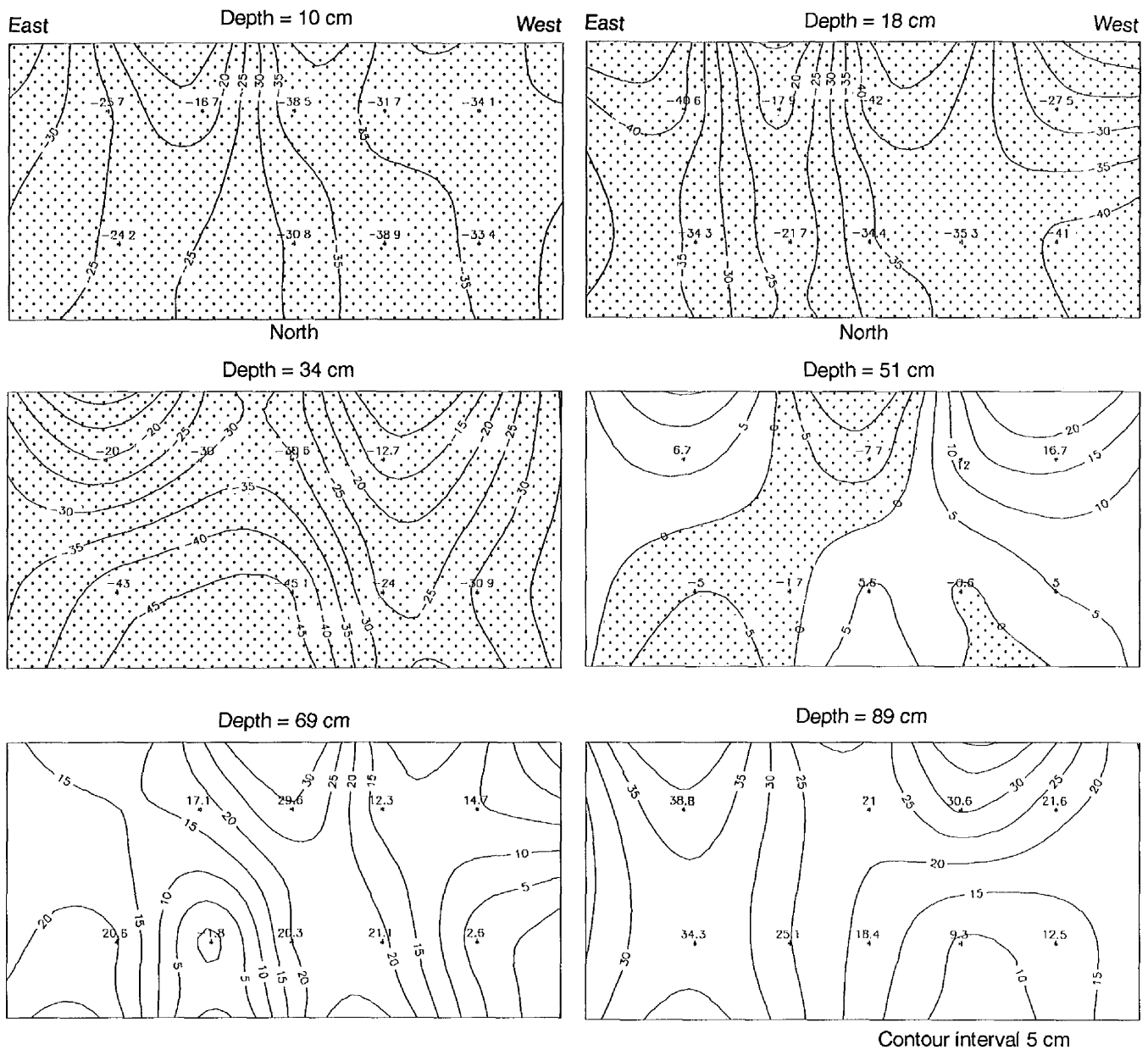
Figure 12 Contour plots of soil tension at six depths in the liner, as averaged for April 1991. Contours were plotted using a minimum curvature technique.

Contour interval 5 cm
Stippled areas indicate tension values less than zero

illustrates the effects of temperature on soil tensions in the column, as monitored by three pressure transducer tensiometers. A relationship between temperature and tension is apparent. As the temperature of the column was decreased, tension values increased. An increase in column temperature produced a corresponding decrease in tension values. The effect that changes in column temperature had on soil tension was quantified by dividing the change in tension by the change in temperature for each phase of the experiment during which the column was cooled. This approach indicated that the effect of temperature on soil tensions was not consistent throughout the column. Temperature effects were greatest in the soil around tensiometer 1 near the "top" of the column (fig. 14), and least in the soil near tensiometer 3 (near the "bottom" of the column). There appeared to be a relationship between the soil tension and the magnitude of change in tension due to temperature changes. The linear regression analysis of the data presented in figure 14 suggested a weak relationship (r^2=0.41). The low
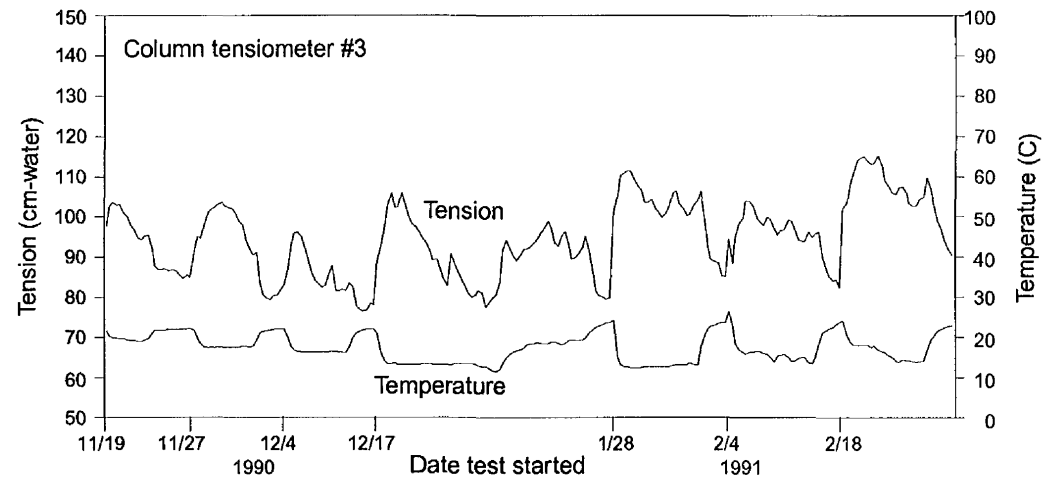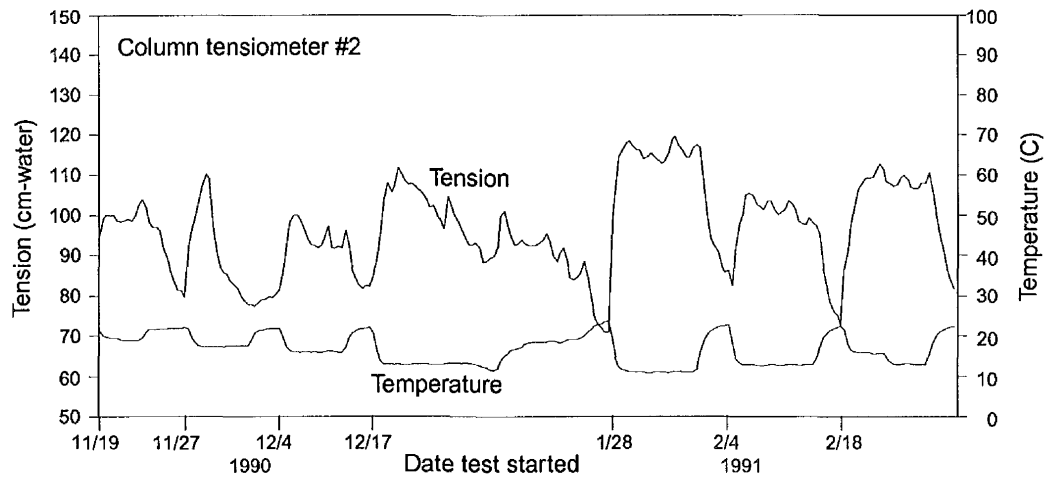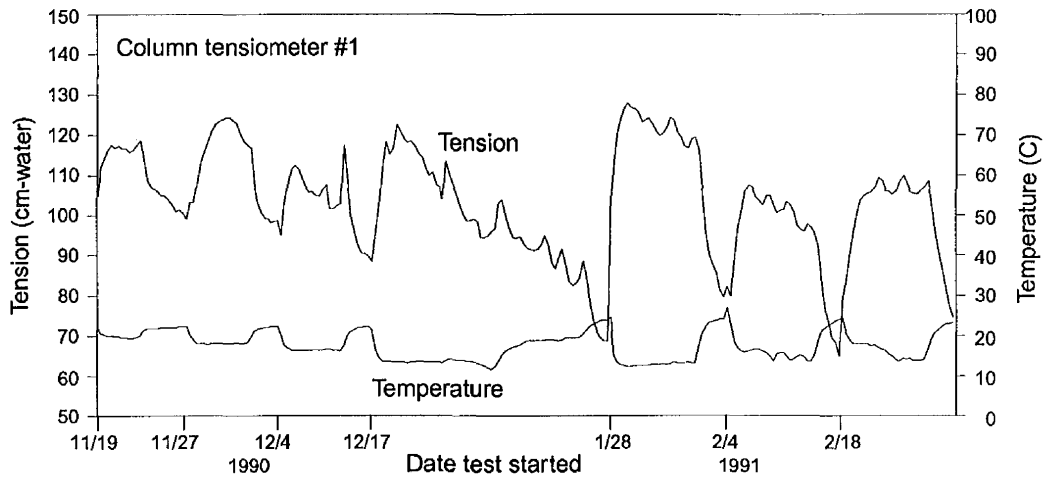
Figure 13 Changes in soil tension due to temperature variations during the soil column experiments. For clarity, data between tests are omitted.
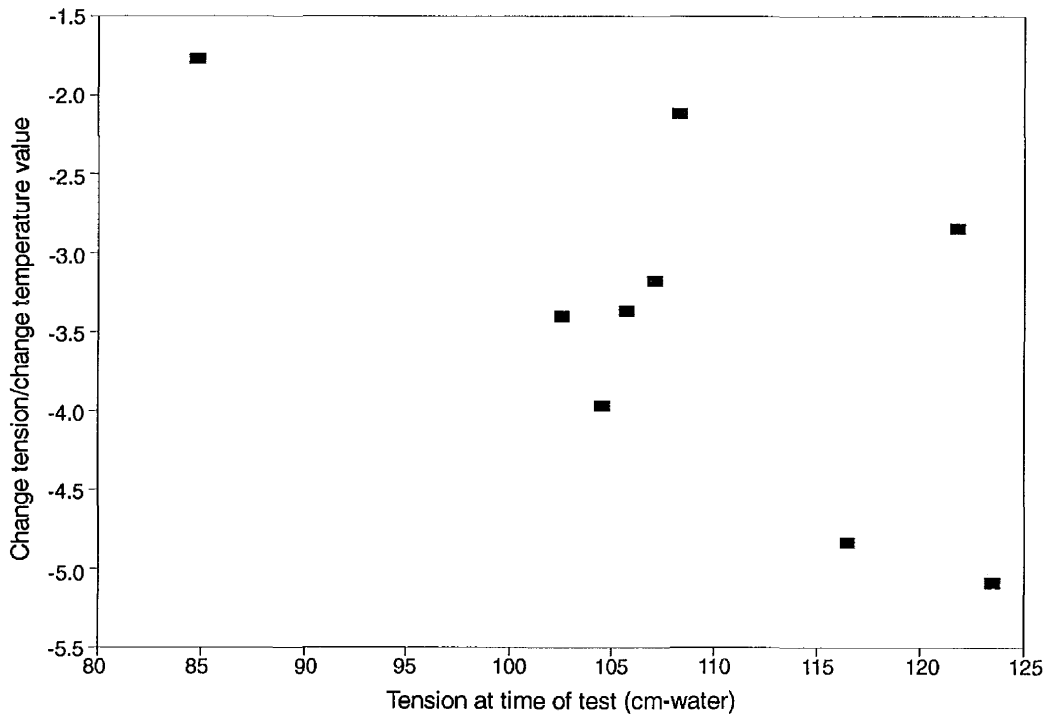
Figure 14 Soil–water tension plotted against change of tension divided by change in temperature for column tensiometer 1.

regression coefficient is due to the two apparent outliers at 105 and 120 cm water tension. Further experimentation is necessary to more precisely define the temperature–tension relationship. The average change in tension per temperature change (Δtension/Δtemperature) was –3.4, –2.8, and –1.4 from the top of the column to the bottom. The experiments also indicated that tension changes tended to be greatest near any tensiometer when soil tension before and during the cooling event was high (drier soil) and least when tension during and prior to the cooling event was low (wetter soil).

Smedema and Zwerman (1967) showed that, when the capillary zone of a soil column contains more than 5% entrapped air, cooling of the column caused a significant lowering of the point at which the pressure head was equal to zero. Their work, based on theory by Peck (1960b), showed an inverse relationship between changes in temperature and soil tension: as temperature decreases tension increases. Turk (1975) suggested that temperature changes have two effects on soil moisture. First, temperature changes effect the surface tension of water; when temperature increases, surface tension decreases and causes water to drain from the soil pores at smaller tension values. Second, temperature changes will cause air entrapped in the soil pores to expand or contract. An increase in air pressure caused by increasing temperature will result in a decrease soil–water tension.

Peck's (1960b) theory of temperature effects on tension was derived from the common gas law PV=nRT. He showed that the volume of entrapped air bubbles will change as soil–water tension and atmospheric pressure change, and that the temperature–pressure effect will be greatest for systems with a large volume of entrapped gas bubbles. Peck's analysis also showed that the effect will be greatest for soils with high moisture content and soils with gradual, rather than steep, moisture characteristic curves. This theory is consistent with what was observed in this study; there was a trend toward greater temperature effects on tension, when tension inside the column was high (fig. 14). Peck's theory may also explain why Δtension/Δtemperature was lowest for the soil located around the tensiometer at the "bottom" of the soil column and greatest in the soil at the "top" of the column. The soil at the bottom of the

East   West

North
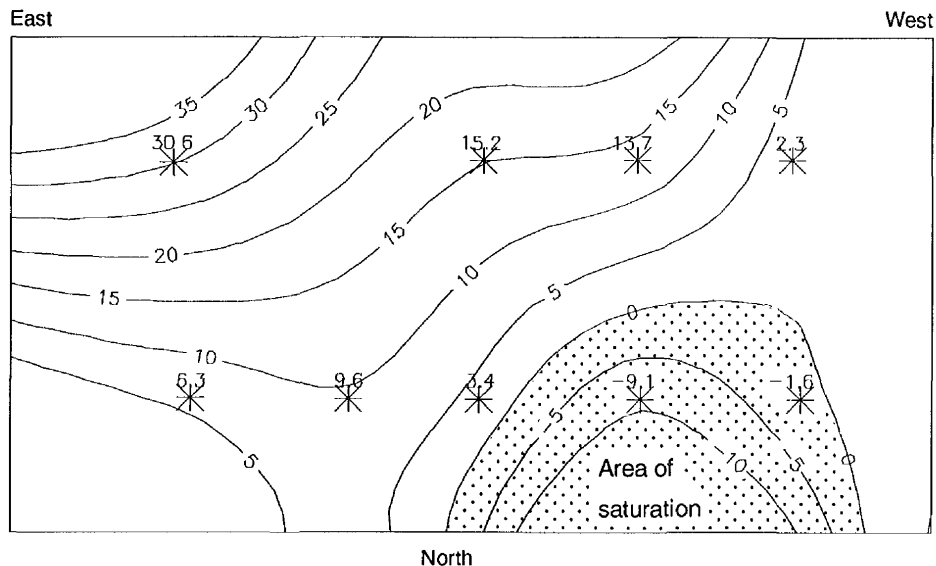
Figure 15 Soil–water tensions plotted at 8.9-cm depth in the liner during the summer of 1991.

column was compacted first; so as additional layers were added, a certain amount of compaction effort was transferred from the preceding lifts to the lower lifts. The additional compaction effort experienced by the lifts toward the bottom of the column may have compacted them more than the upper lifts. The more highly compacted bottom soils have a lower porosity and a higher degree of saturation than the upper soils since the molding water content was the same for all layers. The compounded effect of lower porosity and a greater degree of saturation could result in a more gradual moisture characteristic curve than that for the upper soils. It must be emphasized that the air in the soil must be completely entrapped by the water. If any pathway to the atmosphere exists, then increases in temperature will not cause any corresponding increase in soil gas pressure.

Krapac et al. (1991) questioned whether the fluctuations observed in the liner soil tensions were real or an artifact of some instrument error. The theory discussed here, in combination with the supporting results of the column experiment, appears to explain the tension conditions observed in the liner. As the air is slowly dissolved by the water passing through the liner, the volume of entrapped air will decrease and eventually disappear. The air in the top 10 to 18 cm of the liner appears to have either been displaced or dissolved.

These observations and theory have several potential implications for the movement of water through compacted soil liner systems. This field-scale liner was compacted at about 80% saturation. The low initial tension values for the compacted soil suggest that much of the liner may have been close to tension-saturated at the beginning of the experiment and may not have a "true" wetting front, according to the classic definition of the plane separating the saturated from the unsaturated portions of the soil spectrum. Rather, a zero-tension front separates that portion of the soil where tension changes from positive (unsaturated) to negative (saturated) values. This front has been observed to move up and down in the liner in response to temperature and pressure changes in and around the liner.

During prolonged warm periods, this zero-tension front can migrate to the base of the liner. Several tensiometers on the north side of the liner indicated such an occurrence during the summer of 1991 (fig 15). Soil tensions measured on July 13, 1991, at a depth of 89 cm below the liner surface, ranged from 35 to −10 cm water. (A negative tension value indicates saturated conditions.) A release of water from the underdrains beneath the north half of the liner between June and September 1991 supports the presence of saturated conditions reported by the tensiometers. By September 24, 1991, approximately 7.8 and 4.0 L of water
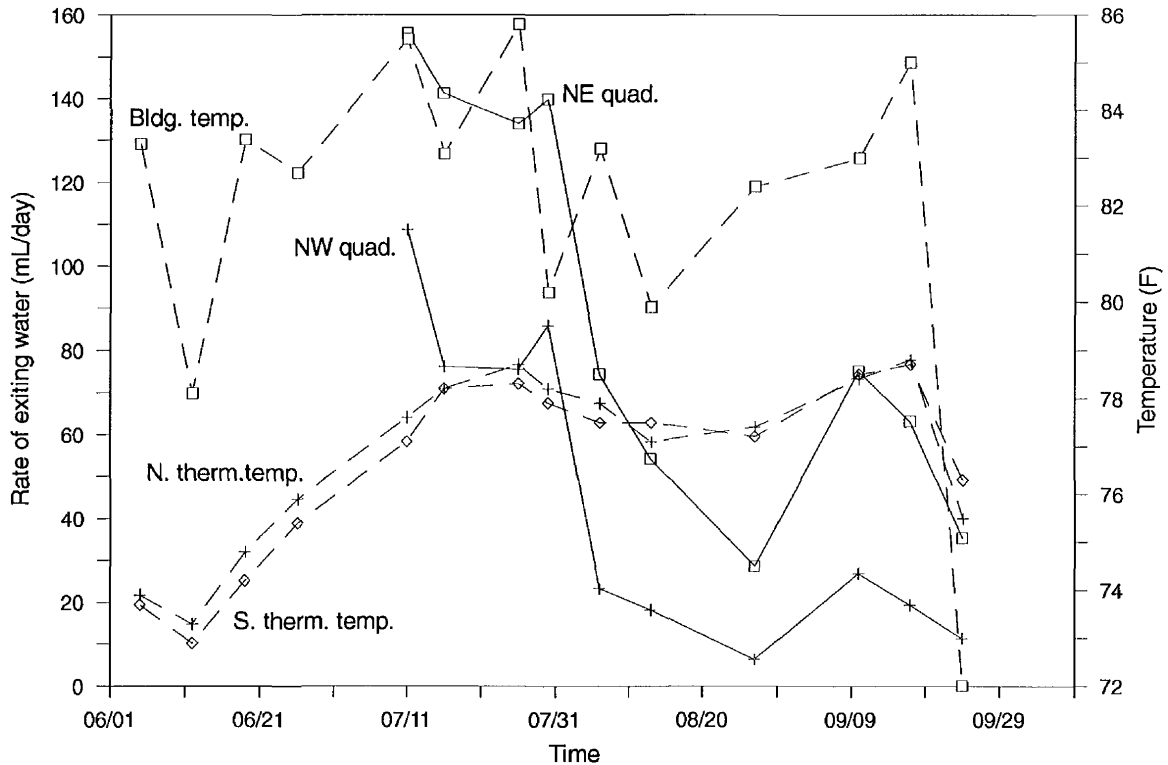
23

Figure 16 Rate of water exiting the bottom of the liner in response to fluctuations in temperature.

had been collected from the northeast and northwest underdrains, respectively. It initially appeared to be breakthrough; however, as the air and liner temperature cooled during the fall and winter, the zero-tension front migrated back towards the middle of the liner and water flow ceased. The long term, monthly averaged tensions for the entire liner at depths of 69 and 89 cm, and possibly 52 cm, indicated unsaturated conditions most of the year.

Temperature of the liner is measured by two thermistors placed in the apron on the east side of the liner. The shelter temperature is also monitored by a thermistor located in the center of the shelter. Comparing the rate at which water is leaving the liner against the temperature of the liner and shelter suggests that temperature affects this exit rate. Large changes in the liner temperature may have been sufficient to cause water to begin breaking through and then cease flowing (fig. 16). A 5° increase in liner temperature occurred between June and July, coincident with water released into the underdrains. More subtle changes in the liner temperature may have effected the rate at which water exited the bottom of the liner. The relatively small (1° to 3°) decrease in liner temperature during the latter part of July and the first half of August caused a decrease in the rate at which water exited the liner. A second increase in temperature (and a corresponding decrease in tension) during late August and early September was again accompanied by an increase in the rate of water exiting the liner. The liner temperature decreased 3° rapidly at the end of September. No water has been observed in the underdrains since September 24, 1991. The summer of 1992 was cool, and no breakthrough occurred.

The release of water from the base of the liner between June and September 1991 may be an effect of higher temperature on entrapped air and soil–water tension. With increasing temperatures, tension will decrease in the lower soil layer of the liner until flow is induced into the underdrain gravel layer. This phenomena is sometimes referred to as the "wick effect." Upon overcoming this tension barrier, water exits the liner until the tension barrier again develops. The occurrence of water exiting the liner will increase and be less dependent on temperature as the lower soil layers of the liner becomes fully saturated.

24

Tritium concentrations in the water collected from the underdrains during 1991 did not increase with time, nor were they higher than tritium concentrations in the liner soil or soil–water samples collected before the addition of tritium to the pond (fig. 17). Tritium concentrations in the water collected from the underdrains varied by less than 7 dpm/mL. Tritium concentrations are expected to increase with time as additional pore volumes of water exit the liner. The addition of tritium approximately 1 year after ponding of the liner may, however, account for the lack of tritium in the underdrain effluent.

Hydraulic Head

Total hydraulic head was computed by subtracting the tensions (shown in fig. 10) from the elevation of the porous cup for each tensiometer. The elevation of the porous cup represents the elevation head; by adding pressure and elevation head, the total hydraulic head can be determined. Heads in the suction lysimeters were determined and compared to head indicated by the pressure-transducer tensiometers. Head in the suction lysimeters was estimated by dividing the volume of water (if any) extracted during initial purging of the instrument by the internal cross-sectional area of the lysimeter tube. This calculation is an estimate of the height of water standing in the lysimeter.

Tensiometer and lysimeter measurements to estimate head in the liner were made on the same day. Figure 18 is a plot of average tensiometer-measured head versus lysimeter-measured head for pairs of instruments located at the same depth in the liner during three sampling events (November 1990, February and June 1991). The line in figure 18 represents equivalent heads between the lysimeters and tensiometers. Heads calculated from the tensiometer data were approximately 1% to 10% lower than those measured by the lysimeters. Coefficients of variation (CV) for heads measured by lysimeters ranged between 1% and 10% for measurements made at the same depth at various locations in the liner. Heads measured by the tensiometers are more variable (CV as large as 40%) than the lysimeters at a given depth in the liner. The relatively good agreement of head measurements between both instruments, and the variability in head exhibited within the liner, suggest the volume of purged water from the lysimeters can be used to verify tensiometer head measurements under saturated conditions.

None of the lysimeters at depths of 69 and 89 cm in the liner contained any purgeable water during the November or February sampling. The lack of water in these lysimeters suggests that the liner was under tension at these depths during this time. In June 1991, however, all but two of the 69-cm-deep lysimeters contained purgeable water; none of the lysimeters at 89 cm contained water. The presence of water in some of the lysimeters at 69 cm suggests zero tension at that depth. According to the lysimeter data, the wetting front (zero tension) may be approaching a depth of 69 cm in the liner as of June 1991 when breakthrough occurred; this depth is 18 cm more than that indicated by the April tensiometer data (fig. 12).

Liner Gradient

The change in total hydraulic head with respect to depth in the liner is the hydraulic gradient. Figure 19 shows liner gradients recorded monthly from before ponding to 3 years after ponding. Gradients were obtained using linear regression analysis with elevation as the independent variable and head as the dependent variable; the slope of the regressed line represents the gradient. Correlation coefficients for this analysis were generally very good, averaging 0.98 and above 0.90 every month except April 1988. The gradient prior to ponding was about 1, corresponding to elevation differences only and indicating little difference in tension with depth. Since tension/head in the top layer of the liner was constant after the second year of monitoring, whereas tension at the base of the liner was fluctuating, gradient also fluctuated (fig. 19). This fluctuation in gradient is seasonal: gradients are higher (median of 1.9) during the winter and lower (median of 1.6) during the summer. This gradient fluctuation affects infiltration rates and causes higher infiltration rates in the winter than in the summer. The average yearly gradients were 1.68, 1.83, and 1.82 for the first, second, and third monitoring years, respectively.
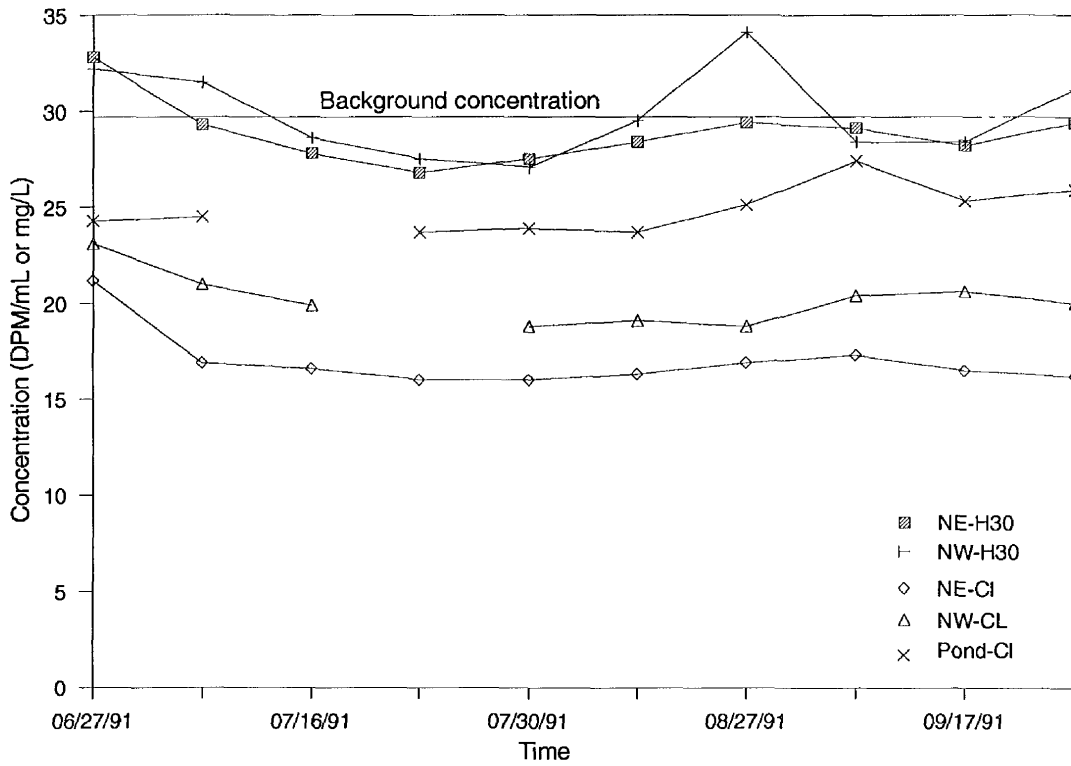
Figure 17 Concentration of tritium in water samples collected from the liner underdrain system.
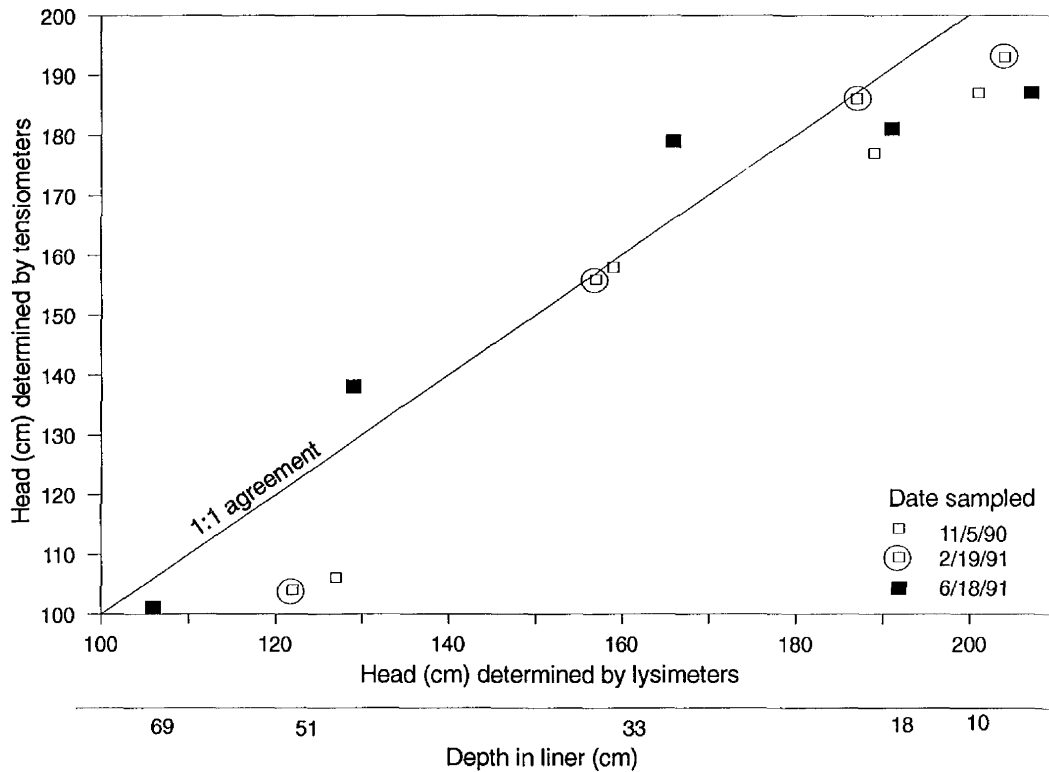

Figure 18 Comparison of head measured by the pressure-transducer tensiometers and the vacuum-pressure lysimeters.

Table 7. Saturated hydraulic conductivity (cm/s) determined from infiltration flux data using Darcy's Law and the Green-Ampt equation.

Method of flux measurement	Analysis period	K_{sat} estimated by Darcy's Law	K_{sat} estimated by Green-Ampt Equation
Large-ring infiltrometers	1st year	3.40×10^{-9}	2.27×10^{-9}
	3rd year	7.25×10^{-9}	8.66×10^{-9}
Small-ring infiltrometers	1st year	4.93×10^{-8}	3.28×10^{-8}
	2nd year	3.50×10^{-8}	3.49×10^{-8}
	3rd year	2.02×10^{-8}	2.41×10^{-8}
Water balance	1st year	4.64×10^{-8}	3.09×10^{-8}
	2nd year	3.66×10^{-8}	3.65×10^{-8}
	3rd year	3.68×10^{-8}	4.39×10^{-8}

Saturated Hydraulic Conductivity

The saturated hydraulic conductivities, which are in close agreement for all monitoring periods (table 7), were calculated by applying Darcy's law and the Green–Ampt equation to the fluxes measured by the small ring infiltrometers. All small ring, hydraulic conductivity values are less than 5.0×10^{-8} cm/s, regardless of the monitoring period or method of calculation. Conductivities determined from the water balance fluxes are generally within a factor of 2 of those conductivities determined by the small ring infiltrometers. In contrast, the large ring infiltrometers have measured conductivities significantly less than those obtained by either the small ring infiltrometers or the water balance approach (table 7). The fluxes and corresponding hydraulic conductivities measured by the large ring infiltrometers have increased during the third year of monitoring and are within approximately two standard deviations of the mean for all infiltration flux data. Consequently, the large ring data for the third year no longer constitute a statistically distinct population.

Solute Diffusion

Soil pore water is collected quarterly from pressure-vacuum lysimeters at various depths in the liner (Krapac et al. 1991). The samples were analyzed for tritium concentration and evaluated with respect to depth and sampling time to determine whether diffusion could be the primary mechanism in the transport of solutes through liner systems. Figure 20 shows the tritium concentration profile in the liner at 168, 475, and 700 days after tritium was added to the liner pond. Because continuous discharge from the base of the liner (breakthrough) has not occurred, elevated tritium has not been observed at the bottom of the liner. Breakthrough curves that depict changes in effluent tritium concentrations are thus not possible to construct.

Support of additional modeling efforts required the use of a one-dimensional, saturated, steady-state flow model (Ogata and Banks 1961, Krapac et al. 1991) to estimate the effective diffusion coefficient of the liner. The calculation of fluid flow was made to equal zero by having the input hydraulic gradient and hydraulic conductivity equal to zero; thus solute movement would be the result of diffusion only. This assumption is valid only if the diffusion transport greatly exceeds the advective transport of water. Various diffusion coefficients were input into the model to compute a theoretical concentration profile. The diffusion coefficient was adjusted until an acceptable fit (by eye) was obtained between the measured concentration profile for the three sampling periods and the theoretical profile (fig. 20). An effective diffusion coefficient for the liner was estimated to be 8.0×10^{-6} cm^2/s. Daniel et al. (1991) found effective diffusion coefficients to range from 1 to 15×10^{-6} cm^2/s for anions (Cl and Br) in a kaolinite and Lufkin clay. Shackelford (1992) reviewed the literature and reported effective diffusion coefficients for "nonreactive" solutes to range from 1.0×10^{-6} to 1.8×10^{-5} cm^2/s in saturated soil, and from 6.3×10^{-7} to 1.5×10^{-5} cm^2/s in unsaturated soils. The effective diffusion coefficient determined for the liner appears to be within the range of values reported in the literature.
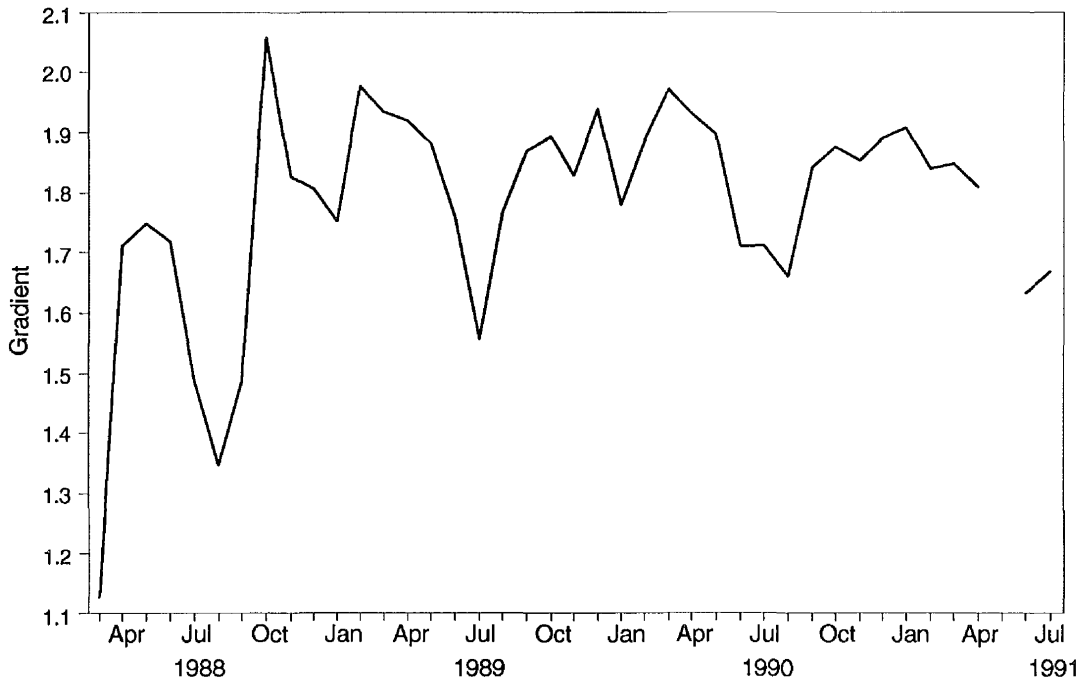
Figure 19 Monthly gradients in the liner.
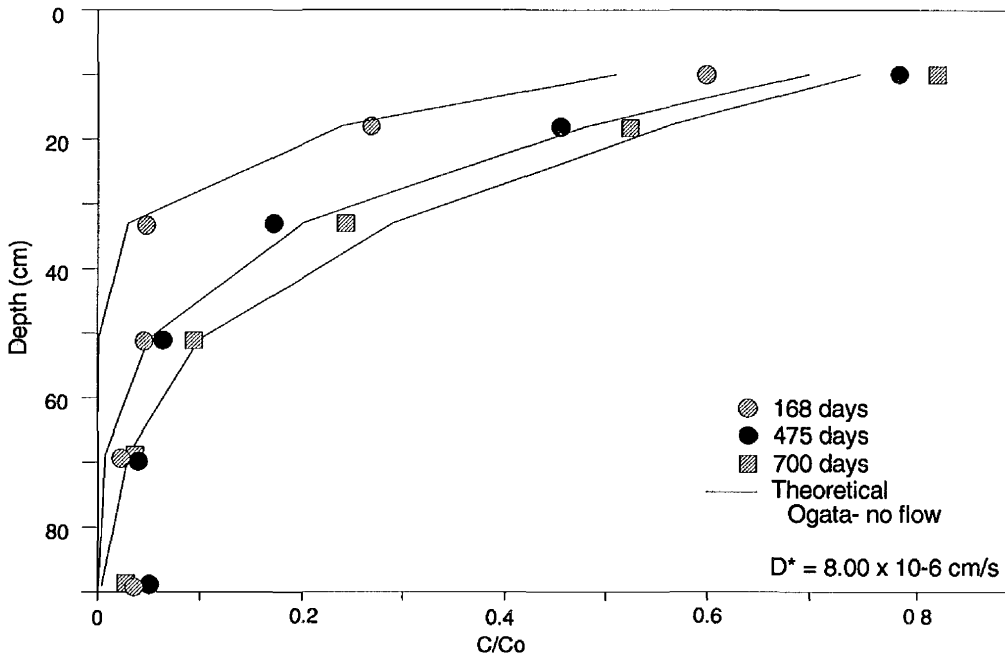
Figure 20 Tritium profiles in the liner.

Transit Time Calculations

Evaluation of analytical and numerical techniques for predicting transit time of water and solutes through soil liners was a project objective. Three simple numerical methods to predict the travel time of water were chosen from seven methods provided by the USEPA (1988). Reasons for selecting the three are discussed in Krapac et al. (1991). The methods include a simple transit time equation, modified transit time equation, and modified Green–Ampt wetting front equation.

Table 8. Calculated transit time using three transit-time equations.

Data set	K_{sat} (cm/s)*	Simple transit equation	Modified transit equation	Modified Green-Ampt Model
SR data geometric mean	2.49×10^{-8}	29.6 years	25.6 years	9.04 years
SR 1**	1.28×10^{-7}	8.52 years	7.36 years	2.60 years
SR 3**	1.15×10^{-7}	9.49 years	8.20 years	2.89 years

* Values used for Green-Ampt equation were calculated from fluxes using the Green-Ampt equation for K_{sat}: SR data = 2.45×10^{-8}, SR 1 = 8.53×10^{-8}, and SR 3 = 7.66×10^{-8}.
** These ring infiltrometers are located in along the northern margin of the northeast quadrant of the liner and have the highest flux of all rings.

Values chosen for parameters in the equations were to simulate the most rapid movement of water though the liner. The saturated hydraulic conductivity used included the geometric mean of the small ring, infiltration flux data and the two highest fluxes from the small ring infiltrometers. It was recognized that these high flux values are located in an area of the liner that may have been affected by construction problems. Effective porosity was used as total porosity (33%), per the USEPA (1988).

The simple transit time equation assumes that the liner has always been saturated and drains freely at the bottom, flow is one dimensional, and steady-state conditions prevail. Simple transit time is calculated by

$$t = \frac{nd}{v} = \frac{nd}{K_{sat}} \frac{d}{(h+d)}$$ (6)

where d is liner thickness (91.0 cm), h is depth of liner pond (31.0 cm), v is Darcian velocity, and n is total porosity (0.33).

The modified transit time equation includes a negative pressure potential at the bottom of the liner. This equation produces a shorter transit time than the simplified transit time equation. It attempts to account for the soil of the liner not being saturated when constructed. The modified transit time is calculated as follows:

$$t = \frac{\eta d}{v} = \frac{\eta d}{K_{sat}} \frac{d}{(h+\psi+d)}$$ (7)

where ψ is the negative pressure potential at the bottom of the liner.

The above equations do not reflect physical reality of a liner that has not yet experienced breakthrough because they do not account for the presence of a wetting front. A more realistic approach (in the case of this liner) is the use of the modified Green–Ampt wetting front equation. Transit time for this equation is predicted from

$$t = \frac{\Theta_s - \Theta_i}{K_{sat}} [L_f - (h+\psi_f)\ln(1 + \frac{L_f}{h+\psi_f})]$$ (8)

where Θ_s is saturated moisture content (0.33), Θ_i is the initial moisture content (0.21), L_f is depth to the wetting front (in this case, the thickness of the liner), and Ψ_f was assumed to be the soil tension just below the wetting front (1 cm). A summary of the transit times calculated from the three equations are presented in table 8.

The Green–Ampt transit time equation appears to provide the most realistic values for transit time in comparison with the other two methods. The temporary appearance in June 1991 of water in the underdrains of the northeast and northwest quadrants of the liner, together with the infiltration fluxes measured (small ring infiltrometers 1 and 3) in these quadrants, formed the basis for comparison of predicted breakthrough and the appearance of water in the under-drains. The travel time of water to reach the bottom of the liner, determined from flux data of small ring infiltrometers 1 and 3, was 2.6 and 2.9 years, respectively. These predictions suggest that breakthrough would occur in late November 1990 or early March 1991. The latter date is approximately 3 months before actual breakthrough in that area.

■ Implications for Liner Performance

The overall performance of the liner from the standpoint of infiltration flux and K_{sat} was successful. The liner has achieved a mean K_{sat} lower that required by the USEPA (i.e., 1×10^{-7} cm/s). In fact, the highest flux value in the data set yields a K_{sat} less than that of the USEPA's limit. Travel times for ponded water moving vertically through the liner are conservatively estimated to be approximately 9.0 years since ponding; however, the high-flux areas affected by construction problems have expected breakthrough times of 2.6 to 2.9 years. (The liner areas that had higher fluxes are not considered to be areas that had flaws caused by construc-tion of the liner. Rather, the high-flux areas were the result of constructing the cutoff wall trench, which allowed lateral forces developed during compaction of the liner to cause slumping into the trench. Trenches such as those used in the experimental liner would not likely be constructed in commercial-scale liners.) The transit time calculations suggest that breakthrough will occur throughout the liner at various times between approximately the fall of 1991 and spring of 1997.

Computer Codes
■ Modeling Using SOILINER

Previous modeling to predict water movement through the large-scale liner had difficulty estimating water fluxes or wetting front movement (Krapac et al. 1991). The failure to accurately simulate moisture movement in the liner was attributed to the inability of the model to predict hydraulic conductivity as a function of soil pressure head (tension). In turn, the inability to predict conductivity may have been the result of initially using a soil moisture characteristic curve constructed for the Batestown till during draining rather than wetting (as in the case of soil in the liner). An additional complication in predicting the conductivity of the liner may be due to the soil hydraulic conductivity decreasing with increasing depth because of enhanced soil compaction and/or the presence of entrapped air in the soil pores. Another attempt has been made to predict water movement through the liner using SOILINER. For this modeling effort, a soil moisture characteristic curve was developed in the laboratory for wetting of the soil.

The modeled predictions of water flux into and out of the liner as well as the movement of the wetting front with respect to time were compared to field-measured fluxes and tensions. None of the model simulations could accurately predict both the fluxes and wetting front depth for the time frame in which the liner has been monitored. Some simulations (5, 6, 9, 14 and 23, table 9) predicted comparable head and zero-tension front profiles, whereas other simulations (1–4, 18, and 22) predicted infiltration fluxes similar to observed. However, those simulations that predicted infiltration fluxes resembling observed results also predicted that the liner should have a significant basal flux before the end of the third year. Because no measurable flux has been observed from the large-scale liner, these simulations appear to be in error. The simulations that accurately predicted the zero-tension front and head profiles for the various time and depth intervals in the liner also predicted infiltration fluxes that were less than one-half of those measured by the small ring infiltrometers.

The continued inability to accurately model moisture movement through the liner may be attributable to several factors. The moisture characteristic curve may still be in error because

Table 9 Flux and wetting front position for the large-scale liner, as predicted by the model SOILINER.

Model Simulation Number	Field Measured Parameters	1	2	3	4	5	6	7	8	9	10
		Model Input Parameters									
Soil Moist. Char. Curve	N/A	A	A	A	A	A	A	A	A	A	12
K_1 (cm/s)	4×10^{-8}	4×10^{-8}	4×10^{-8}	4×10^{-8}	4×10^{-8}	4×10^{-8}	4×10^{-8}	4×10^{-8}	4×10^{-8}	4×10^{-8}	4×10^{-8}
K_2 (cm/s)	N/A	N/A	N/A	N/A	N/A	4×10^{-9}	4×10^{-9}	4×10^{-9}	1.6×10^{-8}	4×10^{-9}	4×10^{-9}
Depth for K change (cm)	N/A	N/A	N/A	N/A	N/A	30	33	27	30	30	30
Porosity	0.33	0.33	0.11	0.33	0.33	0.33	0.33	0.33	0.33	0.40	0.33
Pressure- top of liner	30	30	30	30	30	30	30	30	30	30	30
Pressure-throughout liner	-65	-65	-65	-200	-65	-65	-65	-65	-65	-65	-65
Pressure-bottom of liner	-65	-65	-65	-65	-100	-65	-65	-65	-65	-65	-65
	RESULTS										
	Field Measurements	1	2	3	4	5	6	7	8	9	10
Time 0.3 Years											
Infiltration flux (cm/s)	N/A	8.5×10^{-8}	6.2×10^{-8}	8.5×10^{-8}	9.2×10^{-8}	5.1×10^{-8}	8.3×10^{-8}	4.1×10^{-8}	8.1×10^{-8}	8.9×10^{-8}	1.0×10^{-7}
Effluent flux	0	8.6×10^{-11}	1.1×10^{-10}	1.0×10^{-9}	N/A	5.3×10^{-11}	5.3×10^{-11}	5.3×10^{-11}	6.9×10^{-11}	5.2×10^{-11}	5.4×10^{-11}
Wetting front (cm)	39	27	54	27	23	32	28	31	29	24	18
Time 1 Year											
Infiltration flux (cm/s)	$7.8\text{-}9.2 \times 10^{-8}$	6.0×10^{-8}	5.4×10^{-8}	6.0×10^{-8}	6.4×10^{-8}	1.7×10^{-8}	1.8×10^{-8}	1.7×10^{-8}	3.7×10^{-8}	1.9×10^{-8}	2.3×10^{-8}
Effluent flux	0	1.4×10^{-10}	5.4×10^{-8}	1.0×10^{-9}	N/A	6.3×10^{-11}	6.3×10^{-11}	6.3×10^{-11}	9.7×10^{-11}	6.1×10^{-11}	6.6×10^{-11}
Wetting front (cm)	47	57	83	57	51	43	46	40	54	42	39
Time 2 Years											
Infiltration flux (cm/s)	$6.4\text{-}7.5 \times 10^{-8}$	5.4×10^{-8}		5.4×10^{-8}	5.4×10^{-8}	1.2×10^{-8}	1.3×10^{-8}	1.2×10^{-8}	2.9×10^{-8}	1.4×10^{-8}	1.6×10^{-8}
Effluent flux	0	5.4×10^{-8}		5.4×10^{-8}	5.4×10^{-8}	7.0×10^{-11}	7.0×10^{-11}	7.0×10^{-11}	2.4×10^{-10}	6.8×10^{-11}	7.5×10^{-11}
Wetting front (cm)	50	83		83	83	54	55	51	79	51	46
Time 3 Years											
Infiltration flux (cm/s)	$3.7\text{-}6.7 \times 10^{-8}$					1.1×10^{-8}	1.1×10^{-8}	1.0×10^{-8}	2.7×10^{-8}	1.1×10^{-8}	1.3×10^{-8}
Effluent flux	0					7.6×10^{-11}	7.6×10^{-11}	7.6×10^{-11}	2.7×10^{-8}	7.3×10^{-11}	8.2×10^{-11}
Wetting front (cm)	59					61	63	57	86	57	52
Time 4 Years											
Infiltration flux (cm/s)						9.5×10^{-9}	9.7×10^{-9}	9.3×10^{-9}		1.0×10^{-8}	1.2×10^{-8}
Effluent flux						8.1×10^{-11}	8.5×10^{-11}	8.0×10^{-11}		7.7×10^{-11}	8.8×10^{-11}
Wetting front (cm)						68	71	65		63	57
Time 5 Years											
Infiltration flux (cm/s)						8.8×10^{-9}	8.9×10^{-9}	8.6×10^{-9}		9.3×10^{-9}	1.1×10^{-8}
Effluent flux						1.3×10^{-10}	2.2×10^{-10}	9.8×10^{-11}		8.3×10^{-11}	9.3×10^{-11}
Wetting front (cm)						74	79	71		70	61
Time 6 Years											
Infiltration flux (cm/s)						8.2×10^{-9}	8.3×10^{-9}	8.1×10^{-9}		8.8×10^{-9}	9.9×10^{-9}
Effluent flux						4.9×10^{-10}	4.7×10^{-9}	2.5×10^{-10}		1.3×10^{-10}	1.0×10^{-10}
Wetting front (cm)						82	86	77		74	65

the three samples tested for this analysis were taken from the apron of the liner where wetting and drying may have caused additional compaction. A variety of characteristic curves were modeled, however, and none were able to produce acceptable results.

The model predictions that most closely duplicate observed zero-tension front movement in the liner were obtained when a single reduction in hydraulic conductivity was input into the model at a depth of about 30 cm (simulation 5), or when two reductions in conductivity were input at depths of 15 and 45 cm. The 30-cm depth was determined, based on observed soil tension fluctuation, to be a place in the liner where conductivity could change in response to atmospheric temperature and pressure changes, apparently because of the related expansion and contraction of entrapped air. Poor results were obtained when hydraulic conductivity was input into the model as either a single value or a value gradually decreasing with depth.

Although simulations 5 and 14 were able to reasonably predict the movement of the wetting front in the liner, the predictions of infiltration fluxes in these simulations were generally less than the fluxes observed. One possibility for the discrepancy between observed and predicted fluxes may be that the observed flux measurements are in error. This possibility is remote, however, considering that several different methods of measurement yield the same approximate flux values. It is also possible that the moisture characteristic curve developed in the laboratory is not accurately simulating conditions in the liner. A final explanation may be that there is an error in the model itself, and that the volume of water going into storage (filling dry pores) is too small. (More water going into storage would increase the flux without affecting wetting front movement.) Currently, there is no obvious explanation for the differences in fluxes.

Modeling the downward movement of water through an apparently simple, one-dimensional, unsaturated flow system such as the large-scale liner has been more difficult than expected, despite the large hydrologic database available for this liner project. To accurately model this system may require a multilayer model that could account for two-phase flow and the data that could support such a model. The difficulty in obtaining model predictions similar to observed values suggests that results from simple models for similar systems should be viewed with extreme caution.

CONCLUSIONS

The soil liner experiment is not yet complete. Breakthrough of water and tracer from the base of the liner has not yet occurred; data from this event are essential to determining transit time and testing the accuracy of predictive methods. The study has accomplished most of its goals, however, some of which were enumerated in Krapac (1991b). Principal findings of the study are as follows.

• A soil liner that meets or exceeds the (less than) 1×10^{-7} cm/s hydraulic conductivity standard can be built. Analysis of the liner data to date indicate that the saturated hydraulic conductivity is about 5×10^{-8} or less.

• Appropriate construction practices and quality supervision are essential for successful liner construction. The study showed that preferential flow paths may be present in a liner, even when infiltration measurements indicate that the required level of hydraulic conductivity has been achieved.

• Transit time through the entire liner thickness has not yet been determined. After 3 years of monitoring, the liner is saturated to a depth of more than 51 cm, but less than 69 cm. The apparent wetting front has fluctuated with long term temperature and atmospheric pressure changes. Water discharged from two quadrants of the liner in the summer of 1991; none of the tracers were detected in the discharge water. The discharge may be related to a slumping problem that occurred during construction and that may have resulted in a localized area of higher permeability. The liner areas that had higher fluxes are not considered to be areas that

had flaws caused by construction of the liner. Rather, the high-flux areas were the result of constructing the cutoff wall trench, which allowed lateral forces developed during compaction of the liner to cause slumping into the trench. Trenches such as those used in the experimental liner would not likely be constructed in commercial-scale liners. The Green–Ampt infiltration equation provided the most reliable estimate of transit time for water throughout the liner: about 9 years.

• The liner exhibits very little areal variation in hydraulic properties; only the areas where slumping occurred show any significant differences. A geostatistical analysis of the small ring infiltrometer flux data showed that infiltration flux was unstructured (random) at a scale greater than 1.2 m. Kriged estimates of annual mean infiltration fluxes of the liner quadrants are almost identical to the geometric mean of the measured fluxes.

• Data are insufficient at this time to test the accuracy of predictive models. The model SOILINER was run and appeared not to provide appropriate results. The use of simple one-dimensional models to predict water movement in liner systems needs more work before final conclusions can be drawn.

REFERENCES

Acar, Y. B., and S. D. Field. 1983. Organic leachate effects on the structural stability and hydraulic conductivity of clay liners (proposal). Louisiana State University, Baton Rouge, LA, 11 p.

Albrecht, K. A., and K. Cartwright. 1989. Infiltration and hydraulic conductivity of a compacted earthen liner. Ground Water, v. 27, p. 14–19.

Albrecht, K. A., B. L. Herzog, L. R. Follmer, I. G. Krapac, R. A. Griffin, and K. Cartwright. 1989. Excavation of an instrumented earthen liner: Inspection of dyed flow paths and soil morphology. Hazardous Waste and Hazardous Materials, v. 5, p. 269–279.

Anderson, J. L., and J. Bouma. 1973. Relationships between saturated hydraulic conductivity and morphometric data of an argillic horizon. Soil Science Society of America Proceedings, v. 37, p. 408–413.

Brown, A., S. P. Mathur, and D. J. Kushner. 1989. An orthorhombic bog as a methane reservoir: Global Biochemical Cycles, v. 3, no. 3, p. 205–213.

Brown, K. W., and D. C. Anderson. 1982. Effects of organic solvents on the permeability of clay soils (draft report). Texas A&M University, Texas Agricultural Experiment Station, College Station, Texas, 153 p.

Belanger, T. V., and D. F. Mikutel. 1985. On the use of seepage meters to estimate ground-water nutrient loading to lakes. Water Resources Bulletin, v. 21, no. 2, p. 265–272.

Benjamin, J. R., and C. A. Cornell. 1970. Probability, statistics, and decision for civil engineers. McGraw Hill, New York, p. 466–475.

Cartwright, K., and I. G. Krapac. 1990. Construction and performance of a long-term earthen liner experiment. In Proceedings of Symposium/GT Div./ASCE National Civil Engineering Convention, November 6–7, 1990, San Francisco, CA, p. 135–155.

Chen, H. W., and L. O. Yamamoto. 1987. Permeability tests for hazardous waste management unit clay liners. In D.J.A. van Zyl, S. R. Abt, J. D. Nelson, and T. A. Sheppard (eds.), Geotechnical and Geohydrological Aspects of Waste Management. Lewis Publishers, Chelsea, Michigan, p. 229–244.

Daniel, D. E. 1984. Predicting hydraulic conductivity of clay liners. Journal of Geotechnical Engineering, v. 110, p. 285–300.

Daniel, D. E. 1981. Problems in predicting the permeability of compacted clay liners. Symposium on Uranium Mill Tailings Management, Fort Collins, Colorado, p. 665–675.

Daniel, D. E., C. D. Shackelford, W. P. Liao, and H. M. Liljestrand. 1991. Rate of flow of leachate through clay soil liners. U.S. Environmental Protection Agency, Risk Reduction and Engineering Laboratory, Cincinnati, OH. NTIS PB91-196691, 127 p.

Daniel, D. E., and K. W. Brown. 1988. Landfill liners: How well do they work and what is their future? *In* J. R. Gronow, A. N. Schofield, and R. K. Jain (eds.), Land Disposal of Hazardous Waste. Ellis Horwood Limited, West Essex, England, p. 235–244.

Daniel, D. E., and S. J. Trautwein. 1986. Field permeability test for earthen liners. *In* S. P. Clemence (ed.), Use of In Situ Tests in Geotechnical Engineering. American Society of Civil Engineers, New York, NY, p. 146–160.

Elsbury, B. R., G. A. Sraders, D. C. Anderson, J. A. Rehage, J. O. Sai, and D. E. Daniels. 1990. Field and laboratory testing of a compacted soil liner. U.S. Environmental Protection Agency, Risk Reduction Engineering Laboratory, Cincinnati, OH, EPA/600/S2-88/067, 139 p.

Ely, R. L., G. L. Kingsbury, M. R. Branscome, L. J. Goldman, C. M. Northeim, J. H. Turner, and F. D. Mixon. 1983. Performance of clay caps and liners for disposal facilities (draft). Grant 68-03-3149 to Research Triangle Institute, U.S. Environmental Protection Agency, Cincinnati, OH.

Englund, E., and A. Sparks. 1988. GEO–EAS (geostatistical environmental assessment software) user's guide. U.S. Environmental Protection Agency, Environmental Monitoring Systems Laboratory, Las Vegas, Nevada, Report EPA/600/4-88/033a.

Foreman, D. E. 1984. The effects of hydraulic gradient and concentrated organic chemicals on the hydraulic conductivity of compacted clay. Unpublished M.S. thesis, University of Texas at Austin, 346 p.

Green, W. H., and G. A. Ampt. 1911. Studies on soil physics: I. Flow of air and water through soils. Journal of Agricultural Science, v. 4, no. 1, p. 1–24.

Herzog, B. L., and W. M. Morse. 1986. Hydraulic conductivity at a hazardous waste disposal site: Comparison of laboratory and field determined values. Waste Management and Research, v. 4, p. 177–187.

Johnson, R. A., E. S. Wood, R. J. Wood, and J. Wozmak. 1986. SOILINER model—documentation and user's guide (version 1): EPA/530-SW-86-006, Public Comment Draft, 193 p.

Journel, A. G., and C. J. Huijbregts. 1978. Mining geostatistics. Academic Press, 600 p.

Krapac, I. G., K. Cartwright, B. R. Hensel, B. L. Herzog, T. H. Larson, S. V. Panno, K. H. Rehfeldt, J. B. Risatti, and W. J. Su, and K. R. Rehfeldt. 1991. Construction, Monitoring, and Performance of Two Soil Liners. Illinois State Geological Survey, Environmental Geology 141, 118 p.

Krapac, I. G., K. Cartwright, S. V. Panno, B. R. Hensel, K. H. Rehfeldt, and B. L. Herzog. 1990a. Conductivity and transit time estimates of a soil liner. *In* R. M. Khanbilvardi and T.C. Gooch (eds.), Optimizing the Resources for Water Management. Proceedings of the 17th Annual National Conference, Forth Worth, TX, April 17–21, 1990, ASCE, New York, NY, p. 820–823.

Krapac, I. G., K. Cartwright, S. V. Panno, B. R. Hensel, K. H. Rehfeldt, and B. L. Herzog. 1990b. Water movement through an experimental soil liner. *In* Remedial Action, Treatment, and Disposal of Hazardous Waste—Proceedings of the 16th Annual Hazardous Waste Research Symposium. U.S. Environmental Protection Agency, Risk Reduction Engineering Laboratory, Cincinnati, OH, April 3–5, 1990, EPA/600/9-90 037, p. 263–273

Lohman, S. W., 1972, Ground-water hydraulics. U.S. Geological Survey Professional Paper 708, 21 p.

Mason, D. D., J. F. Lutz. and R. G. Peterson. 1957. Hydraulic conductivity as related to certain soil properties in a number of great soil groups—sampling errors involved. Soil Science Society of America Proceedings, v. 21, p. 554–561.

Mitchell, J. K., and J. S. Younger. 1967. Abnormalities in hydraulic flow through fine-grained soil. Special Technical Publication 417, ASTM, Philadelphia, PA, p. 106–139.

Norum, D. I., and J. N. Luthin. 1968. The effect of entrapped air and barometric fluctuations on the drainage of porous mediums. Water Resources Research, v. 4, no. 2, p. 417–424.

Ogata, A., and R. B. Banks, 1961, A solution of the differential equation of longitudinal dispersion in porous media. U.S. Geological Survey, U.S. Government Printing Office, Washington, DC, Professional Paper 411-A, 7 p.

Olson, R. E., and D. E. Daniel. 1979. Field and laboratory measurements fo the permeability of saturated and partially saturated fine-grained soils. Permeability and Groundwater Contaminant Transport: Symposium. American Society of Testing and Materials, Philadelphia, PA, 67 p.

Panno, S. V., B. L. Herzog, K. Cartwright, K. R. Rehfeldt, I. G. Krapac, and B. R. Hensel. 1991. Field-scale investigation of infiltration into a compacted soil liner. Groundwater, v. 29, no. 6, p. 914–921.

Peck, A. J. 1960a. The water table as affected by atmospheric pressure. Journal of Geophysical Research, v. 65, no. 8, p. 2383–2388.

Peck, A. J. 1960b. Change of moisture tension with temperature and air pressure: theoretical. Soil Science, v. 89, no. 6, p. 303–310.

Quigley, R. M. 1990. Clay barriers for mitigation of contaminant impact: Evaluation and design. *In* Volume II—Clay/Leachate Compatibility Laboratory and Field Diffusion. University of Western Ontario, London, Ontario, Canada, 273 p.

Rogowski, A. S. 1990. Relationship of Laboratory and Field Determined Hydraulic Conductivity in Compacted Layer. U.S. Environmental Protections Agency, Risk Reduction Engineering Laboratory, Cincinnati, OH, EPA/600-2-90/025, 204 p.

Rowe, R. K. 1990. Clay barriers for mitigation of contaminant impact: Evaluation and design. *In* Volume I—Modeling and Its Role in the Geotechnical Design of Barriers. University of Western Ontario, London, Ontario, Canada, 300 p.

Shackelford, C. D. 1992. Laboratory diffusion testing for waste disposal—A review. Journal of Contaminant Hydrology, in press.

Smedema, L. B., and P. J. Zwerman. 1967. Fluctuations of the phreatic surface, 1. Role of entrapped air under a temperature gradient. Soil Science, v. 103, no. 5, p. 354–359.

Smith, R. M., and D. R. Browning. 1942. Persistent water-unsaturation of natural soil in relation to various soil and plant factors. Soil Science Society of America Proceedings, v. 7, p. 114–119.

Turk, L. J. 1975. Diurnal fluctuations of water tables induced by atmospheric pressure changes. Journal of Hydrology, v. 26, p. 1–16.

U.S. Environmental Protection Agency. 1990. Seminars—Design and Construction of RCRA/CERCLA Final Covers. Office of Research and Development, Washington, DC, CERI-90-50, 209 p.

U.S. Environmental Protection Agency. 1988a. Design, Construction, and Evaluation of Clay Liners for Waste Management Facilities. USEPA Risk Reduction Engineering Laboratory, Cincinnati, OH, EPA/530-SW-86-007F.

U.S. Environmental Protection Agency. 1988b. Lining of Waste Containment and Other Impoundment Facilities. USEPA Risk Reduction Engineering Laboratory, Cincinnati, OH, EPA-600/2-88/052, 711 p.

U.S. Environmental Protection Agency. 1987. Hazardous waste management system: Minimum technology requirements, 40CFR part 264 and 265, v. 52, no. 74, p. 12566-1-2569.

U.S. Environmental Protection Agency. 1985. Introduction to Ground-Water Tracers. Robert S. Kerr Environmental Research Laboratory, Ada, OK, EPA/600/2-85/022, 201 p.

U.S. Environmental Protection Agency. 1979. Design and Construction of Covers for Solid Waste Landfills. Municipal Environmental Research Laboratoy, Cincinnati, OH, EPA-600/2-79/165, 249 p.

Zimmie, T. F., J. S. Doynow, and J. T. Wardell. 1981. Permeability testing of soils for hazardous waste disposal sites. Proceedings of the Tenth International Conference on Soil Mechanics and Foundation Engineering, v. 2, Stockholm, Sweden, p. 403–406.

Figure 1 (above) Plan view of the full-scale liner experiment shows the instrument layout. (below) Cross-sectional view shows details of construction; the vertical and horizontal scales are the same.

Figure 2 Design of the column experiment.

Figure 3 Soil moisture characteristic curves.

Figure 4 Volume (in liters) of water infiltration into the liner, as determined from water balance data.

Figure 5 (above) Theoretical curve representing inverse hydraulic gradient as a function of wetting front advancement in the liner. (below) Inverse hydraulic gradient calculated from the infiltration flux data measured for the liner water balance.

Figure 6 Representative cumulative infiltration curve from small ring 6 of infiltrometer 19.

Figure 7 Frequency distribution of infiltration fluxes during the first monitoring year for the ring infiltrometers. Four large ring infiltrometers appear on the far right.

Figure 8 Frequency distribution of infiltration fluxes during the third monitoring year for all ring infiltrometers.

Figure 9 Variograms of infiltration fluxes measured during the first, second, and third year of monitoring by the small ring infiltrometers.

Figure 10 Average monthly tension relative to time at six depths in the liner.

Figure 11 Average monthly temperature and atmospheric pressure in the liner shelter.

Figure 12 Contour plots of soil tension at six depths in the liner, as averaged for the month of April 1991. Contours were plotted using a minimum curvature technique.

Figure 13 Changes in soil tension due to temperature variations during the soil column experiments. For clarity, data between tests are omitted.

Figure 14 Soil–water tension plotted against change of tension divided by change in temperature for column tensiometer 1.

Figure 15 Soil–water tensions at 8.9-cm depth in the liner during the summer of 1991.

Figure 16 Rate of water exiting the bottom of the liner in response to fluctuations in temperature.

Figure 17 Concentration of tritium in water samples collected from the liner underdrain system.

Figure 18 Comparison of head measured by the pressure-transducer tensiometers and the vacuum-pressure lysimeters.

Figure 19 Monthly gradients in the liner.

Figure 20 Tritium profiles in the liner.